

D- π -A compounds with tunable intramolecular charge transfer achieved by incorporation of butenolide nitriles as acceptor moieties

Carlos Moreno-Yruela,[†] Javier Garín,[†] Jesús Orduna,[†] Santiago Franco,[†] Estefanía Quintero,[‡] Juan T. López Navarrete,[‡] Beatriz E. Diosdado,[§] Belén Villacampa,^{||} Juan Casado*[‡] and Raquel Andreu*[†]

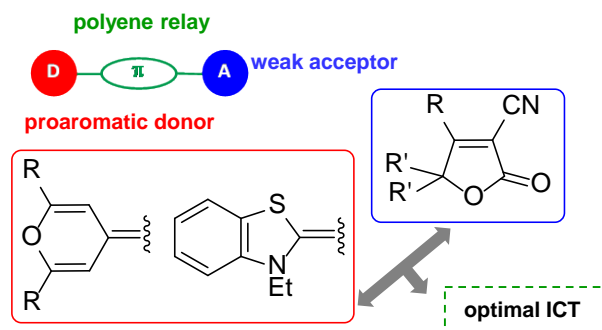
[†] Departamento de Química Orgánica, ICMA, Universidad de Zaragoza-CSIC, 50009 Zaragoza, Spain.

[‡] Departamento de Química Física, Universidad de Málaga, Campus de Teatinos s/n, 29071 Málaga, Spain.

[§] Servicio de Rayos X y Análisis por Fluorescencia, Universidad de Zaragoza, 50009 Zaragoza, Spain.

^{||} Departamento de Física de la Materia Condensada, ICMA, Universidad de Zaragoza-CSIC, 50009 Zaragoza, Spain.

Corresponding author's e-mail address: randreu@unizar.es; casado@uma.es



Abstract

Chromophores where a polyenic spacer separates a 4*H*-pyranylidene or benzothiazolylidene donor and three different butenolide nitriles have been synthesized and characterized. The role of 2(5*H*)-furanones as acceptor units on the polarization and the

second-order nonlinear (NLO) properties has been studied. Thus, their incorporation gives rise to moderately-polarized structures with NLO responses which compare favorably to those of related compounds featuring more efficient electron-withdrawing moieties. Derivatives of the proaromatic butenolide **PhFu** show the best nonlinearities. Benzothiazolylidene-containing chromophores present less alternated structures than their pyranilydene analogues, and, unlike most merocyanines, the degree of charge transfer does not decrease on lengthening the π -bridge.

Introduction

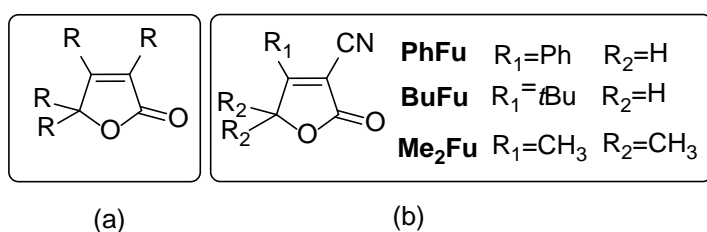
Push-pull organic chromophores, in which a π -conjugated bridge is end-capped by a donor (D) and an acceptor (A), constitute a blueprint in the search for new materials endowed with nonlinear optical (NLO) properties and have been extensively studied because of their technological and fundamental interest.¹ In such D- π -A arrangement, efficient intramolecular charge transfer (ICT) from the donor to the acceptor takes place and the molecules become polarized. Microscopically, the second-order nonlinearity of chromophores can be represented by the scalar product of the vector part of the hyperpolarizability tensor (β) and the dipole moment (μ).

The extent of the ICT can be finely tuned by variations of particular D, π and A components of a push-pull molecule, and this has been demonstrated to be crucial in order to maximize the second-order NLO response. In this way, general structure-activity relationships have been established.²

In simple valence bond language, D- π -A systems can be represented by two extreme limiting forms: neutral (N) and zwitterionic (ZW) with an intermediate situation corresponding to the so-called “cyanine limit” (CL). (Scheme 1)

important $\mu\beta$ value measured by solvatochromic methods and, on the other hand, on a derived LB film. Theoretical calculations also confirm their NLO activity.⁸

Scheme 2. (a) General structure of a 2,3,4,4-tetrasubstituted but-2-ene-4-olide; (b) structures of but-2-ene-4-olide nitriles used in this work.



Butenolide nitriles, with a cyano group in C2 (Scheme 2(b)) could act as weak electron-withdrawing units and, depending on the substitution, offer a double alternative: (i) reacting by the C4 (Scheme 2(b); $R_2 = \text{H}$) they would be incorporated to the chromophore as proaromatic^{4a} acceptors; (ii) reacting by the R_1 position (Scheme 2(b)) they would be linked to the π -spacer as non-proaromatic acceptors and could be considered as a “weak version” of the widely used 2-dicyanomethylene-3-cyano-4,5,5-trimethyl-2,5-hydrofuran (TCF) acceptor.⁹

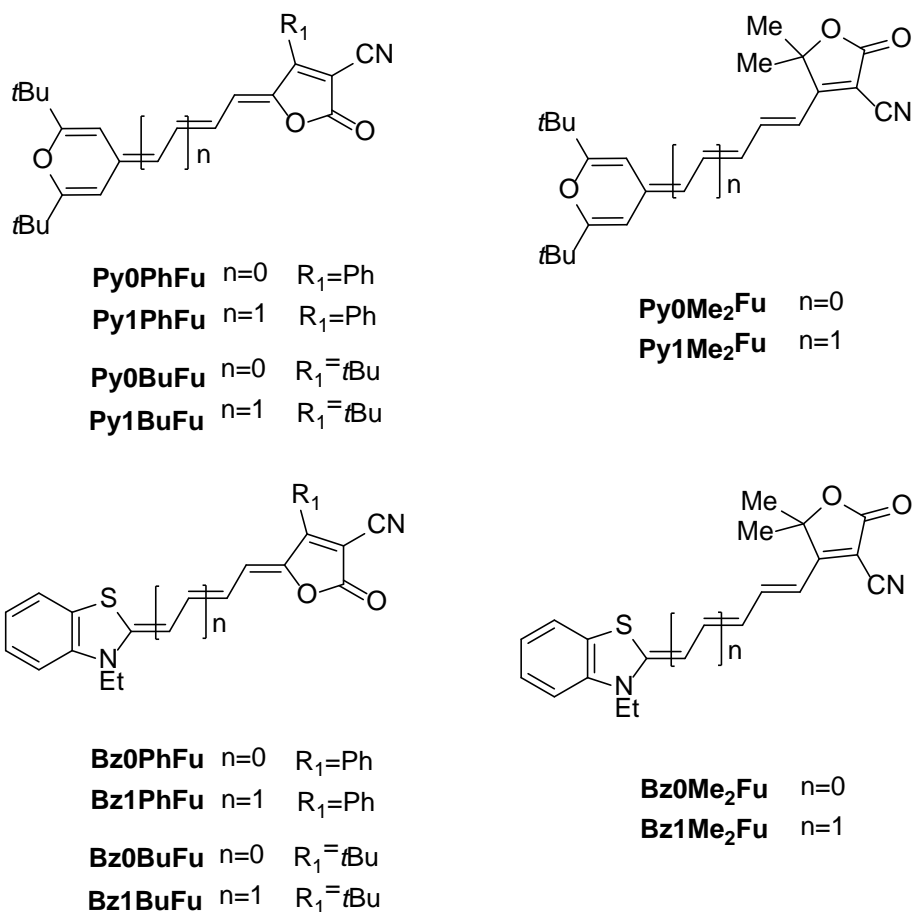
In this context, we have turned our attention to the study of D- π -A compounds with 2(5*H*)-furanones as electron-withdrawing moieties, having second-order NLO responses. Thus, three butenolide-type acceptors have been chosen for this work (Scheme 2(b)): compounds **PhFu** and **BuFu** are proaromatic acceptors and differ on the R_1 substituent: a phenyl (**PhFu**) or a *tert*-butyl group (**BuFu**). The latter have a double purpose: first, to disclose the effect of an inductive-donor and bulky substituent on the electron-withdrawing unit, and second, to increase the solubility of the final chromophores. 2(5*H*)-furanone **Me₂Fu** is a non proaromatic acceptor. Overall, this will allow to evaluate the effect that the

quinoid or non-quinoid character of the acceptor moiety has on the molecular polarization and on the NLO response of the final D- π -A systems.

With the aim of ensuring an effective molecular polarization, compounds **PhFu**, **Me₂Fu**, **BuFu** have been combined (Scheme 3) with a polyene relay and two proaromatic electron-donor moieties: 4*H*-pyranylidene¹⁰ (series **Py**) and benzothiazolylidene¹¹ (series **Bz**). The latter fragment has also been studied as acceptor¹² or π -spacer¹³ in chromophores with NLO properties.

For the sake of clarity, target compounds (Scheme 3) have been named beginning with **Py** or **Bz**, in order to indicate the donor, followed by a number (**0** or **1**) that denotes the length of the π -spacer and **PhFu**, **Me₂Fu**, **BuFu** that concerns the butenolide ring.

Scheme 3. Structures of the target compounds.



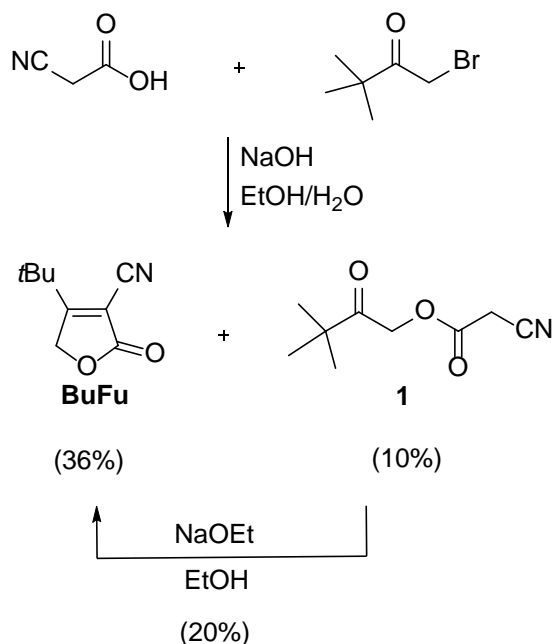
A detailed investigation of the ICT **existent** in these chromophores by using different techniques, together with the measurement of their $\mu\beta$ figure of merit is presented throughout this paper.

Results and Discussion

Synthesis. The synthesis of acceptors **PhFu**, **Me₂Fu**, **BuFu** was previously reported^{14–16} with a different method for each butenolide. Our attempts to prepare **BuFu** according a **previously described method**¹⁶ led to the desired compound, but not with successful yield. Then, for this work, compound **BuFu** was synthesized by following the experimental protocol used for **PhFu** (Scheme 4), starting from 1-bromopinacolone and cyanoacetic

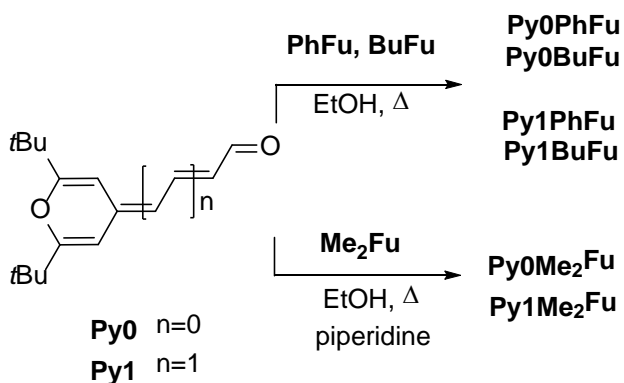
acid, and was been fully characterized. During this synthesis, the corresponding oxo-cyanoacetate **1** was also isolated and characterized. Subsequent cyclization of **1** in the presence of base afforded another portion of furanone **BuFu**. (Scheme 4)

Scheme 4. Synthesis of butenolide nitrile BuFu.



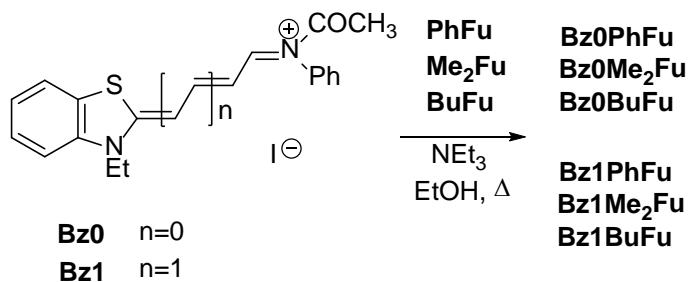
For series **Py**, the Knoevenagel reaction between acceptors **PhFu**, **Me₂Fu**, **BuFu** and pyranlylidene-containing aldehydes **Py0–Py1**^{17,10b} in EtOH afforded the new D- π -A chromophores **Py0(PhFu,Me₂Fu,BuFu)** and **Py1(PhFu,Me₂Fu,BuFu)** in yields that ranged from 20 to 69%. (Scheme 5) For the reactions involving furanone **Me₂Fu**, the addition of one drop of piperidine was needed. It is noteworthy that yields for derivatives **Py0(PhFu,Me₂Fu,BuFu)** were considerably higher than for their vinylogues **Py1(PhFu,Me₂Fu,BuFu)**. This is due to the fact that during the synthesis of the latter, small amounts of **Py0(PhFu,Me₂Fu,BuFu)** are formed as a consequence of a vinylene-shortening reaction that has already been reported for other Knoevenagel-type reactions by us¹⁸ and other authors.¹⁹

Scheme 5. Synthesis of pyranylidene-containing chromophores $\text{Py0}(\text{PhFu}, \text{Me}_2\text{Fu}, \text{BuFu})$ and $\text{Py1}(\text{PhFu}, \text{Me}_2\text{Fu}, \text{BuFu})$.



Concerning compounds $\text{Bz0}(\text{PhFu}, \text{Me}_2\text{Fu}, \text{BuFu})$ and $\text{Bz1}(\text{PhFu}, \text{Me}_2\text{Fu}, \text{BuFu})$, they were synthesized as shown in Scheme 6, by reaction of iminium salts Bz0-Bz1^{20} with the corresponding acceptors PhFu , Me_2Fu , BuFu in the presence of triethylamine. In this series no vinylene-shortening degradation was detected.

Scheme 6. Synthesis of benzothiazolyidene-containing chromophores $\text{Bz0}(\text{PhFu}, \text{Me}_2\text{Fu}, \text{BuFu})$ and $\text{Bz1}(\text{PhFu}, \text{Me}_2\text{Fu}, \text{BuFu})$.



The synthesis of compound Bz0PhFu had already been reported¹⁴ using piperidine as base, but not fully characterized. Moreover, its NLO response had been previously studied by other authors^{8a} as mentioned in the Introduction.

Structural characterization by X-ray crystallography. Single crystals of compounds **Py0PhFu**, **Py1PhFu** and **Py1Me₂Fu** were obtained by slow diffusion of hexane into a solution of the corresponding chromophore in CH₂Cl₂ at room temperature. Four crystallographically independent molecules are found in the asymmetric unit cell of **Py0PhFu** (Figure 1), while those of **Py1PhFu** and **Py1Me₂Fu** both contain a single molecule. (Figure 2)

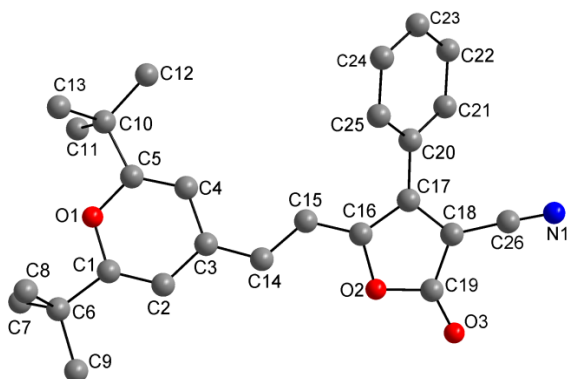
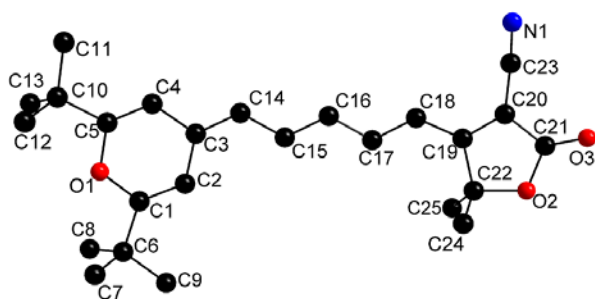


Figure 1. Molecular structure of compound **Py0PhFu**. (For clarity, only one molecule is shown. See Figure S-38 for viewing the four molecules found in the asymmetric unit cell)



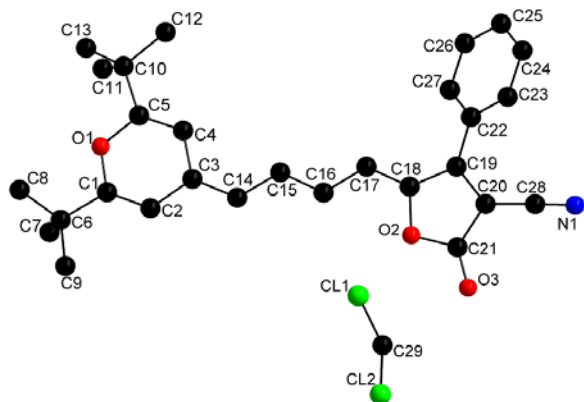
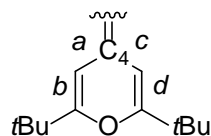


Figure 2. Molecular structures of compounds **Py1PhFu**, which crystallizes with a molecule of CH_2Cl_2 (bottom), and **Py1Me₂Fu** (top).

The analysis of the solid state structures can provide useful information about how the ground electronic state polarization varies when modifying the character of the butenolide group or lengthening the spacer.

There are some main features shared by the three structures: (i) the D- π -A system is essentially planar with the following angles between the mean planes of the pyran and the butenolide rings (**Py0PhFu**: 17.3°, 6.0°, 16.9°, 6.0°, **Py1PhFu**: 5.5°, **Py1Me₂Fu**: 10°); (ii) the phenyl substituent in **Py0PhFu–Py1PhFu** is not coplanar with the butenolide moiety (dihedral angles: 37.4°, 45°, 36.7° and 44.6° for the four molecules in **Py0PhFu** and 33.3° in **Py1PhFu**); (iii) the polyenic chain has an all-*trans* geometry except for the formal double bond connecting the π -spacer with the acceptor unit in **Py0PhFu–Py1PhFu**, with a *Z* configuration.

Some structural parameters of the pyranilidene ring, including BLA value along the spacer (Figure 3) reveal the ground electronic state polarization from the donor end of the chromophore to the acceptor group.



Bond lengths involved
in the calculation of δr

Compd	C–O ^a	C ₄ –C _{exo} ^a	δr	I_6	BLA ^a
Py0PhFu ^b	1.372	1.391	0.094	34.2	0.023
Py1PhFu	1.374	1.386	0.098	32.3	0.030
Py1Me₂Fu	1.374	1.354	0.113	27.8	0.056

^a Bond length in Å

^b Average values for the four molecules

Figure 3. Structural parameters for the pyranylidene donor and BLA values.

Then, for compounds **Py0PhFu–Py1PhFu**, a shortening of C–O bond, together with a lengthening of the pyran exocyclic bond and a decreased degree of C–C bond alternation (evaluated through the parameter δr ,²¹ $\delta r = (a-b+c-d)/2$; $\delta r=0$ for benzene and 0.10 for fully quinoid rings) was found. Moreover, the Bird index (I_6)²² of the donor (Figure 3), used as an estimation of the aromaticity of the ring ($I_6 = 25.4$ for fully quinoid pyrans; $I_6 = 50$ for pyrylium cations^{10b}) also indicates the partial contribution of the zwitterionic form to the ground **electronic** state of derivatives **Py0PhFu–Py1PhFu**.

Furthermore, comparison of structural parameters (Figure 3) shows that compound **Py0PhFu** presents a more polarized structure than its vinilogue **Py1PhFu**.

Comparison with X-ray structures of merocyanines bearing other acceptors could be instructive to get more information about the ground **electronic** state polarization of the studied systems. For instance, analogues of **Py0PhFu/Py1PhFu** with 3-phenyl-5-isoxazolone^{10b}/1,1,3-tricyano-2-phenylpropene^{10b} or 2-dicyanomethylenethiazole^{10c} respectively as acceptor end show a BLA value close to zero. This indicates that

incorporation of acceptor **PhFu** leads to moderately-polarized structures, and this fact may have a positive effect on the NLO behavior (see NLO section) as it places compounds **Py0PhFu–Py1PhFu**, at least in the solid state, far from the cyanine limit. In this context, structure of **Py1PhFu** is similar to that of its recently reported 2-dicyanomethylenethiophene²³ analogue.

The structural parameters for **Py1Me₂Fu** (Figure 3) indicate a limited polarization of the donor unit given that the δr parameter and the C₄–C_{exo} bond length (C3=C14 bond in **Py1Me₂Fu**, see Figure 2) both exhibit values corresponding to a fully quinoid 4H-pyranylidene ring. In fact, 1.354 Å is even shorter than the C₄–C_{exo} bond in 2,2',6,6'-tetraphenylbipyranlydene (1.385 Å) taken as reference for a quinoidal derivative.²⁴ On the other hand, BLA value for **Py1Me₂Fu** is 0.056 Å (Figure 3), which locates the chromophore in the region where β is maximized due to an optimal degree of mixing between neutral and charge-separated canonical forms.²⁵

Moreover, comparison of the structural parameters of **Py1PhFu/Py1Me₂Fu**, with a proaromatic/non proaromatic furanone as acceptor fragment respectively indicates that **Py1Me₂Fu** presents a more alternated structure.

Concerning series **Bz**, single crystals of derivative **Bz0PhFu** were obtained by slow diffusion of propan-2-ol into a solution of the chromophore in CH₂Cl₂ at room temperature. Compound **Bz0PhFu** crystallizes in the monoclinic space group P21/c, and some of the main features of this structure are similar to those of the described above. For this compound, another X-ray structure has been previously reported, different from the structure submitted here: it claims a P-1 space group, incorporating a CHCl₃ crystallized molecule.²⁶ Both structures have the same geometric configurations.

In our structure, BLA value is -0.005 \AA , indicating that this chromophore is close to the cyanine limit in the solid state, and therefore located in region C of Marder's plot.^{3b} This data also accounts for a more polarized structure than its analogue **Py0PhFu** (BLA = 0.023, Figure 3) pointing out to a better electron-donating ability of the benzothiazole moiety compared to that of the pyranilidene ring. This behavior is in agreement with the trend followed by octupolar merocyanine dyes designed for two-photon absorption (TPA) with these donors.²⁷

A complete description of the crystal structure is reported in the Supporting Information (SI), section 5.

CCDC-1407292 (**Bz0PhFu**), CCDC-1407293 (**Py0PhFu**), CCDC-1407294 (**Py1Me₂Fu**) and CCDC-1407295 (**Py1PhFu**) contain the supplementary crystallographic data for this paper. These data can be obtained free of charge from The Cambridge Crystallographic Data Centre.

¹H NMR Studies. ¹H NMR spectroscopy affords valuable information about both the geometry and the ground electronic state polarization of the chromophores herein studied. Concerning their stereochemistry, analysis of ³J_{HH} coupling constants indicates an all-*trans* geometry along the spacer, with ³J_{HH} values ranging from 14.9 to 13.4 Hz for the –CH=CH– bonds and from 13.1 to 11.6 Hz for the =CH–CH= bonds. This stereochemistry mimics those observed by X-ray diffraction for compounds **Py0PhFu**, **Py1PhFu**, **Py1Me₂Fu**, **Bz0PhFu**.

Regarding the ground electronic state polarization of the studied compounds, the analysis of ΔJ values (defined as the difference between the averaged ³J_{HH} values of the double and single bonds along the polymethine chain)²⁸ for **Py1(PhFu,Me₂Fu,BuFu)**, obtained from spectra registered in CDCl₃ (1.0 Hz, 2.3 Hz and 1.5 Hz respectively), indicates that

polarization increases in the order **Py1Me₂Fu** < **Py1BuFu** < **Py1PhFu**, which reveals the fact that quinoidal butenolides (**PhFu**, **BuFu**) are better electron-withdrawing groups than non-quinoidal **Me₂Fu**. For **PhFu** (with a phenyl group) and **BuFu** (with the *tert*-butyl substituent), the former presents a higher electron-withdrawing character.

For the analysis of the benzothiazolylidene derivatives, see SI, section 3, Figure S25.

Finally, for all chromophores, the chemical shifts of the H atoms along the spacer show the typical oscillatory behavior²⁹ that reflects the alternation in the electron density of the carbon atoms to which H's are bonded: *e.g.*, for **Py1BuFu**, starting from pyranilydene donor group, in CDCl₃ 5.68, 7.08, 6.59, 6.73 ppm.

Calculated Structures. The molecular geometries of all chromophores were optimized at the CPCM-M06-2X/6-31G* level in dichloromethane, starting from configurations depicted in Scheme 3 which are supported by crystallographic and spectral data. The resulting **theoretical** structures were nearly planar.

Analysis of natural bond orbital (NBO) atomic charge on various molecular domains (Table 1) allows a deeper understanding of the polarization of the molecules.

TABLE 1. Calculated NBO charges on various molecular domains from the optimized CPCM-M06-2X/6-31G* molecular geometries (in CH₂Cl₂).

Compd	Donor	π -spacer	Acceptor
Py0PhFu	+0.371	+0.005	-0.376
Py0Me₂Fu	+0.340	-0.054	-0.286
Py0BuFu	+0.340	-0.007	-0.333
Py1PhFu	+0.324	+0.027	-0.351
Py1Me₂Fu	+0.297	-0.034	-0.263
Py1BuFu	+0.297	+0.008	-0.305
Bz0PhFu	+0.465	-0.059	-0.406
Bz0Me₂Fu	+0.432	-0.131	-0.301

Bz0BuFu	+0.436	-0.072	-0.364
Bz1PhFu	+0.421	-0.043	-0.378
Bz1Me₂Fu	+0.394	-0.114	-0.280
Bz1BuFu	+0.397	-0.067	-0.330

In general, the positive charge is concentrated on the donor ring and the negative charge on the acceptor moiety, although in the **Bz** series, the π -spacer supports a slight negative charge, more important for derivatives **Me₂Fu**.

For both series (**Py** and **Bz**) comparison of compounds that only differ in the acceptor group shows that polarization of the chromophores increases in the order **Me₂Fu**<**BuFu**<**PhFu**, in agreement with ¹H NMR data and X-ray studies (**Py1PhFu**/**Py1Me₂Fu**), thus confirming the higher electron-withdrawing ability for butenolide **PhFu**.

For a given D/A pair, lengthening the conjugated spacer with a vinylene unit leads to a decrease in the charge of the end groups and, in consequence, to more alternated structures, in line with the findings from the X-ray analysis (**Py0PhFu**/**Py1PhFu**).

Finally, comparison of the charges between analogous chromophores of the **Py** and **Bz** series shows that **the latter** are more polarized than their **Py** analogues, indicating a major contribution of the zwitterionic form to the ground state, as it has been shown by the crystallographic study of **Py0PhFu**/**Bz0PhFu**.

Electrochemistry. The redox properties of target chromophores together with acceptors **PhFu**, **Me₂Fu**, **BuFu** were studied by cyclic voltammetry (CV) in CH₂Cl₂ and the results are gathered in Table 2.

TABLE 2. Electrochemical data^a and E_{HOMO} and E_{LUMO} values theoretically calculated.^b

Compd	E_{ox} (V)	E_{red} (V)	E_{HOMO} (eV)	E_{LUMO} (eV)
PhFu		-1.23		
Me₂Fu		-1.85		
BuFu		-1.74		
Py0PhFu	+0.89	-0.98 ^{c,a}	-6.56	-2.35
Py0Me₂Fu	+0.93	-1.17 ^{c,e}	-6.61	-2.10
Py0BuFu	+0.86	-1.09 ^{c,a}	-6.51	-2.19
Py1PhFu	+0.64	-0.82 ^{c,f}	-6.29	-2.49
Py1Me₂Fu	+0.64	-1.02 ^{c,f}	-6.33	-2.26
Py1BuFu	+0.59	-0.94 ^{c,e}	-6.25	-2.34
Bz0PhFu	+0.84	-1.15	-6.46	-2.18
Bz0Me₂Fu	+0.79	-1.38	-6.50	-1.90
Bz0BuFu	+0.82	-1.31	-6.41	-2.01
Bz1PhFu	+0.56	-1.02	-6.20	-2.36
Bz1Me₂Fu	+0.55	-1.20	-6.23	-2.12
Bz1BuFu	+0.48	-1.12	-6.16	-2.20

^a 10^{-3} M in CH_2Cl_2 versus Ag/AgCl (3 M KCl), glassy carbon working electrode, Pt counter electrode, 20 °C, 0.1 M NBu_4PF_6 , 100 mV s^{-1} scan rate. Ferrocene internal reference $E^{1/2} = +0.46$ V ($\Delta E_p = 0.13$ V). ^b Calculated at the CPCM-M06-2X/6-311+G(2d,p)//CPCM-M06-2X/6-31G* level in CH_2Cl_2 . ^c Reversible reduction wave ($E^{1/2}$). ^d $\Delta E_p = 0.13$ V. ^e $\Delta E_p = 0.12$ V. ^f $\Delta E_p = 0.11$ V.

Voltammograms for acceptors **PhFu, Me₂Fu, BuFu** show an irreversible reduction wave. Values of E_{red} depend on the type of the furanone. Thus, the non-proaromatic acceptor **Me₂Fu** presents the highest $|E_{\text{red}}|$ data. For proaromatic acceptors **PhFu, BuFu**, the presence of a *tert*-butyl group in C4 implies a lower electron-withdrawing ability with higher $|E_{\text{red}}|$ for **BuFu** compared to **PhFu**.

All D- π -A systems show one oxidation and one reduction waves corresponding to the donor moiety and the acceptor unit, respectively. Reduction process for the series **Py** is reversible. When E_{red} data are compared in both **Py** and **Bz** series, results follow the same trend encountered for the isolated acceptors, *i.e.* the reduction process is easier in the order: systems **Me₂Fu** < systems **BuFu** < systems **PhFu**, thus confirming the superior electron-withdrawing effect of acceptor **PhFu**, in agreement with ¹H NMR study, crystal structures (**Py1PhFu/Py1Me₂Fu**) and theoretical data. Inspection of calculated E_{LUMO} data indicates that derivatives of acceptor **PhFu** have the lowest values. On the other hand, E_{ox} values are also influenced by the acceptor fragment, being compounds derived from **BuFu** (except **Bz0BuFu**) the most easily oxidized. E_{HOMO} data are in agreement with this observed trend.

Moreover, for a given acceptor, it can be seen that both oxidation and reduction processes become easier on chain lengthening (for example cf. **Py0PhFu/Py1PhFu**; **Bz0PhFu/Bz1PhFu**), pointing out to a weaker interaction between the donor and acceptor ends. In line with this analysis, compounds **0** show higher calculated gaps than their vinylogues **1**.

Comparison of compounds **Py** with their analogues of series **Bz** shows lower (higher) oxidation (reduction) potentials for the latter, pointing out to the higher electron-donating ability of the benzothiazole moiety. This result is in agreement with the literature data.³⁰ Furthermore, the observed trends in E_{ox} and E_{red} are also confirmed by theoretical calculations, which show that both E_{HOMO} and E_{LUMO} values increase on passing from pyran derivatives **Py** to their benzothiazole **Bz** counterparts.

Vibrational spectroscopy.

Infrared (IR) spectroscopy can afford useful information about the degree of ground state polarization of the merocyanines herein studied.^{10c,23,31} Thus, the stretching vibration

frequencies of the C≡N and C=O bonds are sensitive to the increasing electron density on them, downshifting upon ground state polarization. Indeed, taking the isolated acceptors **PhFu**, **Me₂Fu**, **BuFu** as references (Table 3), the $\nu(\text{C}\equiv\text{N})$ and $\nu(\text{C}=\text{O})$ frequency values of **Py0(PhFu,Me₂Fu,BuFu)**, **Py1(PhFu,Me₂Fu,BuFu)**, **Bz0(PhFu,Me₂Fu,BuFu)** and **Bz1(PhFu,Me₂Fu,BuFu)** appear at significantly lower frequencies, affirming the polarization from the donor to the butenolide group.

TABLE 3. Infrared data (measured on nujol suspension; data in cm⁻¹).

Compd	$\nu(\text{C}\equiv\text{N})$	$\nu(\text{C}=\text{O})$	Compd	$\nu(\text{C}\equiv\text{N})$	$\nu(\text{C}=\text{O})$
PhFu	2231	1752			
Me₂Fu	2239	1769			
BuFu	2238	1776			
Py0PhFu	2213	1739	Bz0PhFu	2207	1722
Py0Me₂Fu	2206	1738	Bz0Me₂Fu	2210	1723
Py0BuFu	2215	1746	Bz0BuFu	2209	1720
Py1PhFu	2217	1742	Bz1PhFu	2200	1729
Py1Me₂Fu	2201	1742	Bz1Me₂Fu	2213	1739
Py1BuFu	2219	1749	Bz1BuFu	2191	1702

Table 3 reveals two different trends concerning the dependence of $\nu(\text{C}\equiv\text{N})$ on chain lengthening. Thus, for pyranilidene-containing chromophores (**Py** series), increasing the length of the polyenic spacer gives rise to a frequency upshift of $\nu(\text{C}\equiv\text{N})$ (also for $\nu(\text{C}=\text{O})$ values), except for **Py0Me₂Fu** and **Py1Me₂Fu** ($\nu(\text{C}\equiv\text{N})$). This reveals a decreased polarization (and zwitterionic character) for the longer derivatives **1**, in agreement with calculated data and X-ray (**Py0PhFu/Py1PhFu**).

On the other hand, lengthening the spacer in the series **Bz** leads to a frequency downshift of the $\nu(\text{C}\equiv\text{N})$ vibration (compounds **Bz0Me₂Fu**– **Bz1Me₂Fu** have similar values), which suggests a higher zwitterionic character for the longer derivatives. This behavior may be related to the more extended conjugation path, which facilitates polarization of the π system towards the butenolide end and, although this trend is uncommon, some examples are reported.^{10c,11e,32}

The lower frequencies of both $\nu(\text{C}\equiv\text{N})$ and $\nu(\text{C}=\text{O})$ bands in series **Bz** compared to those of series **Py** (derivatives of furanone **Me₂Fu** do not fulfill this trend for the $\text{C}\equiv\text{N}$ bond, see below discussion about Raman spectroscopy) show the stronger electron-donating ability of the benzothiazole group in relation to the pyranilidene one, as disclosed by computational studies and X-ray (**Py0PhFu**/ **Bz0PhFu**).

Figure 4 shows the Raman spectra of the studied compounds. The $\nu(\text{C}\equiv\text{N})$ in compound **Py0PhFu** appears at 2214 cm^{-1} and shifts to 2210 cm^{-1} in **Bz0PhFu**, reaffirming the greater electron donor ability of the latter. The corresponding $\nu(\text{C}=\text{O})$ appears at 1736 cm^{-1} in **Py0PhFu** and 1708 cm^{-1} in **Bz0PhFu**. This frequency downshift on **Bz0PhFu** is related with a larger contribution of the enolic structure **C** upon charge polarization, (Scheme 7) which is consistent with the five member ring viewed as an aromatic furan and substituted at the β position (α in the furanone ring) by the cyano group. This aromaticity gain upon polarization favors a greater delocalization of the charge on the carbonyl group. In this regard, the cyano is placed in a cross conjugated fashion constraining its electron-withdrawal character.

On increasing the length of the C=C/C–C spacer from **Bz0PhFu** to **Bz1PhFu** the $\nu(\text{C}\equiv\text{N})$ band shifts as $2210\text{ cm}^{-1} \rightarrow 2202\text{ cm}^{-1}$, whereas $\nu(\text{C}=\text{O})$ Raman band is not detected, likely due to the strong enolic character that dramatically decreases its Raman intensity, as it is typical of alcoholate compounds. This situation is in agreement with an important increase of the contribution of the C type canonical form (Scheme 7) for compound **Bz1PhFu** further indicating that, by lengthening the π -spacer in series **Bz** a more polarized structure results. In contrast, in **Py** series, given their weaker electron-donating character, a frequency upshift behavior is observed. Moreover, the bands at 1652 (**Py0PhFu**) and 1665 (**Py1PhFu**) cm^{-1} are due to the $\nu(\text{C}=\text{C})$ modes in the pyranilidene moieties.

The replacement of the phenyl group in β position of the furanone by a *tert*-butyl one does not change the main tendencies (downshifts of the $\nu(\text{C}\equiv\text{N})$ and $\nu(\text{C}=\text{O})$ Raman frequencies, on passing from **Py0BuFu** to **Bz0BuFu** and from **Bz0BuFu** to **Bz1BuFu**) observed for the phenyl substituted series. For derivatives **0**, different trends depending on the donor are observed: for pyranilidene derivatives, frequencies upshift from **Py0PhFu** to **Py0BuFu**, due to the strong steric crowding that the *tert*-butyl group exerts on the vinylene bridge, that weakens the donor-acceptor coupling (Figure 5).

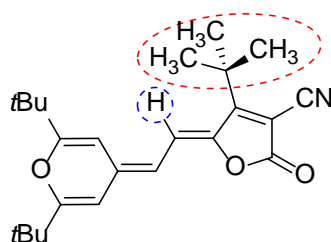


Figure 5. Crowding effect of the *tert*-butyl group that decreases the molecular polarization (chromophore **Py0BuFu**).

On the other hand, for benzothiazolylidene systems **Bz0PhFu** and **Bz0BuFu**, the frequencies scarcely change.

For chromophores bearing butenolide **Me₂Fu**, a canonical form similar to C in Scheme 7 does not longer exist, and the acceptor part of the molecule can be viewed as an acceptor with a cyano and an ester groups, placed one after the other, in a cross-conjugated fashion, and therefore competing for the negative charge. Given the disposition of the two groups, the cyano, with a slightly stronger electron-withdrawing character than the ester, should have a preferential situation to drain charge from the bridge. This can be the reason for the lower frequency for the $\nu(\text{C}\equiv\text{N})$ band in **Py0Me₂Fu** (2209 cm^{-1}) compared to **Py0PhFu** (2214 cm^{-1}). On the other hand, the $\nu(\text{C}=\text{O})$ frequencies scarcely change due to the lack of enolic character (form C in Scheme 7), which is compensated by the inductive effect of the oxygen in the ester. These two trends are also observed in the IR data (Table 3).

For derivative **Bz0Me₂Fu**, the $\nu(\text{C}=\text{O})$ bands undergo significant upshifts regarding **Bz0PhFu** or **Bz0BuFu**, which further reaffirm the isolation of the carbonyl groups in a position unaffected by the charge polarization (fully gathered by the nitriles).

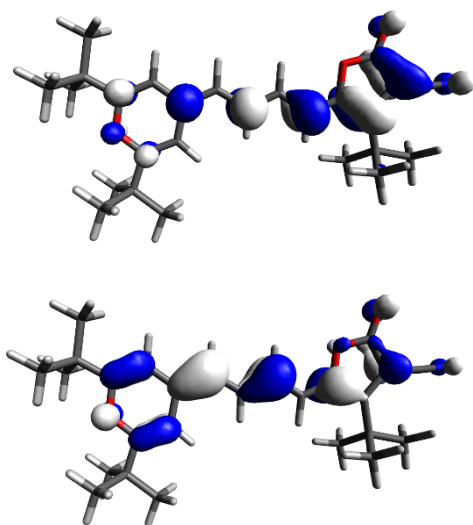
Overall, the replacement of **PhFu**, **BuFu** units as acceptors by furanone **Me₂Fu** involves a decrease in the polarization of the final chromophores.

A study of the frequency behavior of the $\nu(\text{C}\equiv\text{N})$ and $\nu(\text{C}=\text{O})$ bands in the oxidized and reduced forms according to the redox processes in the CV is also carried out and presented in the SI file, section 6.

UV-Vis Spectroscopy. The UV-vis absorption data of push-pull systems in solvents with different polarity are collected in Table 4. All chromophores show very strong and broad electronic absorption bands within the visible region, with structured bands in some of the solvents studied. (See spectra in the SI).

Electron densities related to frontier orbitals (see topologies for **Py1BuFu** chosen as the model compound in Figure 6 and for the rest of the chromophores in SI) are mainly supported by the donor unit and its nearest polyenic fragment for the HOMO, and by the butenolide ring in the case of LUMO.

Figure 6. Illustration of the HOMO (bottom) and LUMO (top) of compound **Py1BuFu**.



TD-DFT calculations (CPCM-M06-2X/6-311+G(2d,p)//CPCM-M06-2X/6-31G* level in CH_2Cl_2) describe the first excited state as a consequence of a one-electron transition from the HOMO to the LUMO. The large HOMO-LUMO overlap is responsible for the strength of the absorption bands.

TABLE 4. UV-Vis data^a

Compd	λ_{\max} (log ϵ) 1,4-dioxane	λ_{\max} (log ϵ) CH ₂ Cl ₂	λ_{\max} (log ϵ) DMF
Py0PhFu	503 (sh)	519 (sh)	518 (sh)
	536 (4.71)	559 (4.79)	558 (4.79)
	568 (sh)	591 (4.81)	597 (4.85)
Py0Me₂Fu	491 (4.56)	499 (sh)	498 (sh)
	515 (4.57)	532 (4.69)	529 (4.70)
	553 (sh)	568 (4.57)	563 (sh)
Py0BuFu	487 (sh)	505 (sh)	506 (sh)
	513 (4.68)	539 (4.79)	544 (4.75)
	554 (sh)	573 (sh)	580 (sh)
Py1PhFu	589 (4.63)	585 (sh)	589 (sh)
		635 (4.73)	638 (4.71)
		684 (sh)	692 (4.63)
Py1Me₂Fu	538 (4.63)	585 (4.70)	575 (4.69)
		644 (sh)	
Py1BuFu	551 (4.47)	599 (4.50)	598 (4.47)
			679 (sh)
Bz0PhFu	529 (sh)	538 (sh)	538 (sh)
	566 (4.80)	576 (5.10)	579 (5.10)
Bz0Me₂Fu	521 (4.74)	523 (sh)	524 (sh)
	541 (4.78)	553 (4.93)	559 (4.97)
Bz0BuFu	521 (sh)	529 (4.75)	533 (4.72)
	550 (4.85)	564 (5.10)	567 (5.67)
Bz1PhFu	611 (sh)	628 (sh)	634 (sh)
	642 (4.59)	678 (5.00)	687 (5.23)
Bz1Me₂Fu	585 (4.46)	596 (sh)	596 (sh)
		634 (4.78)	644 (4.84)
Bz1BuFu	594 (4.67)	618 (4.86)	623 (sh)
		656 (5.00)	669 (5.12)

^a All λ_{\max} data in nm.

Comparison of series **0** and **1** indicates that the λ_{\max} values increase on lengthening the spacer, effect **that** is more accentuated in CH₂Cl₂ or DMF than in the less polar 1,4-dioxane. Taking as model pairs **Py0PhFu/Py1PhFu** and **Bz0PhFu/Bz1PhFu**, this

augmentation reaches ~100 nm,³³ pointing to weakly alternated structures, more polarized in the case of **Bz** derivatives (102 nm, 0.32 eV in CH₂Cl₂; 108 nm, 0.34 eV in DMF) than in **Py** systems (0.29 eV both in CH₂Cl₂ and DMF). This trend is in agreement with other experimental techniques (IR, Raman, CV, **Py0PhFu/Bz0PhFu** X-ray) and calculated NBO charges.

When different furanones are compared, λ_{\max} decreases in the following order **PhFu**>**BuFu**>**Me₂Fu**. This behavior can be explained, on the one hand, by the character (quinoid or non-quinoid) of the acceptor moiety. Thus, the presence of the quinoid ring causes a red shift of the maximum absorption wavelength in derivatives **PhFu, BuFu** when compared to their analogues **Me₂Fu** (e.g., 23 nm (0.08 eV) for **Py0PhFu/Py0Me₂Fu** and 5 nm (0.02 eV) for **Py0BuFu/Py0Me₂Fu**, both in CH₂Cl₂). On the other hand, the replacement of the phenyl ring in compounds **PhFu** for a *tert*-butyl group in derivatives **BuFu** gives rise to a hypsochromic shift (e.g., 85 nm (0.26 eV) for **Py1PhFu/Py1BuFu** and 22 nm (0.06 eV) for **Bz1PhFu/Bz1BuFu**, both in CH₂Cl₂). The same effect was observed for cyanine dyes bearing a 4*H*-pyran-4-ylidene moiety.³⁴ The order above mentioned suggests a parallel decrease in the corresponding acceptor strengths (**PhFu**>**BuFu**>**Me₂Fu**), in line with the results of ¹H NMR spectroscopy, theoretical data and CV.

In general, derivatives of **Bz** series present λ_{\max} values lower than their **Py** analogues,²⁷ although for systems **1** this trend is not observed for all the solvents studied. Moreover, **Bz** systems show larger ϵ values than their **Py** equivalents, and for some solvents, values beyond 10⁵ were found, in agreement with other benzothiazolylidene- π -A chromophores previously reported.^{11c,11e, 27,35}

Concerning the dependence of the band position on solvent polarity, positive solvatochromism in low polarity solvents (*cf.* dioxane and CH₂Cl₂) is observed for all chromophores. On the other hand, when data in CH₂Cl₂ and DMF are compared, the bathochromic shift encountered becomes smaller for derivatives **PhFu/BuFu**, whereas for compounds **Me₂Fu**, solvatochromism found depends on the donor unit: slightly negative for **Py** derivatives³⁶ and positive for **Bz** systems.

Nonlinear Optical properties. The second-order nonlinear optical properties of chromophores herein studied were measured by electric field-induced second harmonic generation (EFISHG) in dichloromethane at 1907 nm, and the zero-frequency $\mu\beta_0$ values were calculated by using the two-level model.³⁷ In the case of the benzothiazolylidene systems (series **Bz**), the lowest energy absorption band, which is the more intense one for each compound, has been used. Given that for derivatives of **Py** series the lowest energy bands in some of the spectra became weak shoulders (indistinguishable in some of the longest compounds), in order to compare $\mu\beta_0$ values in this series, the high intensity central band has been considered (Table 5). For the sake of comparison, Disperse Red 1, a common benchmark for organic NLO chromophores shows a $\mu\beta_0$ value of ca. 490×10^{-48} esu and 425×10^{-48} in CH₂Cl₂ and DMF respectively, under the same experimental conditions.

TABLE 5. Experimental and calculated NLO Properties

Compd	$\mu\beta^a$ (10^{-48} esu)	$\mu\beta_0^b$ (10^{-48} esu)	$\mu\beta^c$ (10^{-48} esu)
Py0PhFu	950	575	521
Py0Me₂Fu	800	510	395
Py0BuFu	850	530	499

Py1PhFu	2850	1420	2125
Py1Me₂Fu	2100	1190	1798
Py1BuFu	1800	990	1801
Bz0PhFu	560	325	580
Bz0Me₂Fu	520	320	477
Bz0BuFu	^d	-	531
Bz1PhFu	3300	1440	2136
Bz1Me₂Fu	2900	1430	1838
Bz1BuFu	2600	1210	1797

^a $\mu\beta$ values determined in CH₂Cl₂ at 1907 nm (experimental uncertainty less than $\pm 15\%$, except for **Bz0PhFu–Bz0Me₂Fu** ($\sim 20\%$)). ^b Experimental $\mu\beta_0$ values in CH₂Cl₂ calculated using the two-level model. ^c Calculated at the HF/6-31G*//CPCM-M06-2x/6-31G* level in CH₂Cl₂. ^d For this compound a reliable value cannot be provided due to its instability in CH₂Cl₂ during the time of measurements.

As it has been already observed for other NLO-chromophores previously studied, lengthening the polyenic chain by a single vinylene unit gives rise to an important increase in the NLO response, which is remarkably pronounced for series **Bz**: $\mu\beta_0(\mathbf{Bz1PhFu})/\mu\beta_0(\mathbf{Bz0PhFu}) = 4.4$ and $\mu\beta_0(\mathbf{Bz1Me_2Fu})/\mu\beta_0(\mathbf{Bz0Me_2Fu}) = 4.5$.

Regarding the influence of acceptor structure on the NLO properties of the studied chromophores, derivatives of the proaromatic butenolide nitrile **PhFu** have the best NLO responses (for **Bz0PhFu–Bz0Me₂Fu** almost the same value was obtained).

Comparison of analogous compounds in **Py** and **Bz** series reveals that, for derivatives **0**, pyranilydene-containing chromophores show higher $\mu\beta_0$ values than their related benzothiazolydene systems. Different experimental techniques (*e.g.* IR, Raman, CV)

showed a more polarized character for benzothiazolylidene chromophores, due to the higher electron-donating ability of the benzothiazole moiety compared to the pyran one. Thus, the change **Py** → **Bz** in the more polarized shorter derivatives **0** results in a decreased NLO response, approaching the region B/C of the Marder's plot.^{3b} For **1** derivatives, NLO responses are similar for **Py** and **Bz** systems (with furanone **PhFu**) or even higher for the latter (with acceptors **Me₂Fu** and **BuFu**).

Measurements in DMF were also performed for model compounds **Py1PhFu** and **Py1Me₂Fu**. The following experimental values (10^{-48} esu) were found: chromophore **Py1PhFu**: 1700 ($\mu\beta$), 700 ($\mu\beta_0$); chromophore **Py1Me₂Fu**: 910 ($\mu\beta$), 530 ($\mu\beta_0$). Results show a decline of $\mu\beta_0$ in both cases, compared to those measured in dichloromethane (Table 5), indicating that these systems are left-handed chromophores (A/B region), with the neutral form predominating in this solvent polarity range.

The calculated $\mu\beta_0$ values (HF/6-31G*, Table 5) are in reasonably good consonance with the experimental ones, and they essentially reproduce the trends experimentally observed in terms of the effects of the acceptor **PhFu** and the length of the polyenic chain. Concerning the influence of the donor group, theoretical calculations do not predict the experimental observed effects for series **0**, although differences are generally small.

Finally, it could also be instructive to compare the NLO properties of the compounds herein reported to those of related derivatives featuring other acceptor moieties, including those previously mentioned in the X-ray section (See Figures 7 and 8 and Table 6).

Figure 7: Structures of related chromophores to series **Py0** previously reported.

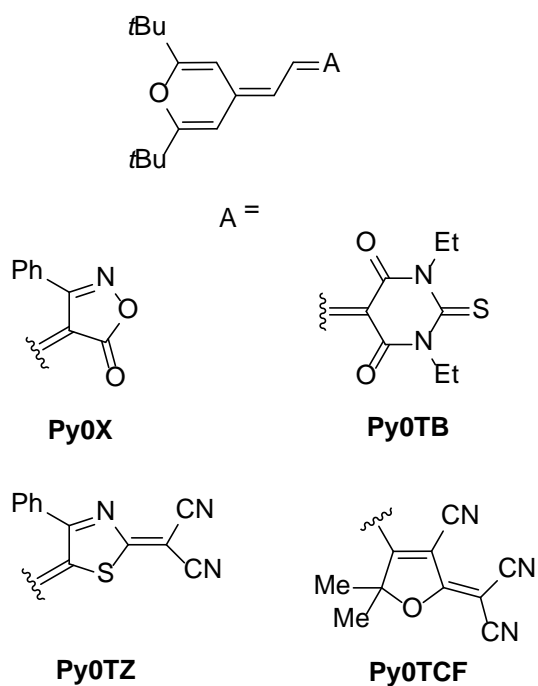


Figure 8: Structures of related chromophores to series **Py1** previously reported.

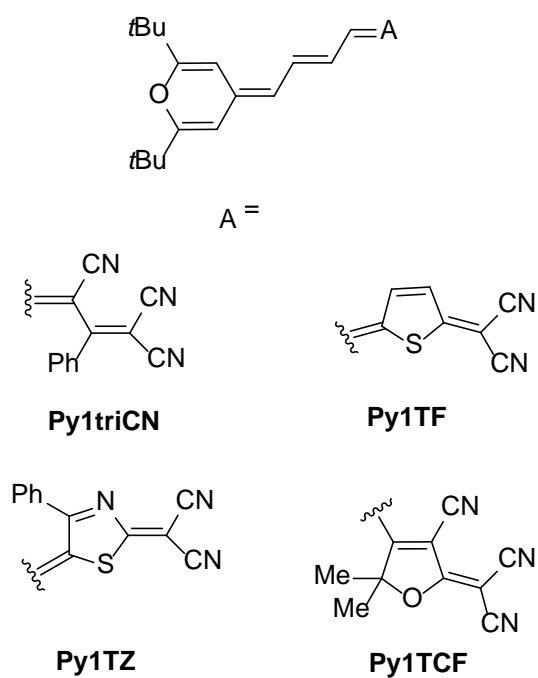


TABLE 6. NLO Properties for related chromophores to series Py

Compd	Ref.	$\mu\beta_0^a$ (10^{-48} esu)	λ_{\max}^b (nm)
Py0X	10b	+64	
Py0TB	10b	-60	
Py0TZ	10c	-450	
Py0TCF	10b	+310	592, 639
Py1triCN	10b	+670	
Py1TF	23	+1370	658, 709, 788
Py1TZ	10c	-1010	
Py1TCF	10b	+1520	675, 740

^a Experimental $\mu\beta_0$ values in CH_2Cl_2 calculated using the two-level model from $\mu\beta$ measured by EFISHG at 1907 nm.

^b In CH_2Cl_2 .

Thus, analogue of **Py0PhFu** with 3-phenyl-5-isoxazolone as acceptor,^{10b} **Py0X** shows a lower $\mu\beta_0$ value than **Py0PhFu**, in agreement with a more polarized structure in solution, apart from the solid state (See X-Ray section). Other chromophores with powerful electron-withdrawing ends have also lower nonlinearities than **Py0PhFu**, even negative figure of merit, as in the case of the thiobarbiturate derivative **Py0TB**.^{10b}

In the same way, **Py1triCN** with 1,1,3-tricyano-2-phenylpropene,^{10b} has a lower response than **Py1PhFu**, in line with a less alternated structure in solution (also in the solid state, as disclosed by X-ray crystallography).

Series with a 2-dicyanomethylenethiazole moiety^{10c} as end group (**Py0TZ**, Figure 7 and **Py1TZ**, Figure 8) show negative values of $\mu\beta_0$, being essentially zwitterionic molecules that show negative solvatochromism. Nevertheless, absolute values are slightly lower compared to those of **Py0PhFu** and **Py1PhFu** respectively.

As it has been stated in the X-ray section, **Py1PhFu** and its equivalent with 2-dicyanomethylenethiophene²³ **Py1TF** have similar structures, and it is noteworthy that **Py1PhFu**, while being more transparent (Table 4), shows even slightly higher NLO response.

The pyranilidene-derived Fischer carbene complexes reported by Caro,^{10a,38} with the same length of the π -relay than the chromophores herein studied show lower $\mu\beta_{1907}$ values than those of compounds **Py0(PhFu,Me₂Fu,BuFu)** and **Py1(PhFu,Me₂Fu,BuFu)**.

On the other hand, as it has been mentioned in the Introduction, furanone **Me₂Fu** can be viewed as a “weak version” of the efficient TCF acceptor, and thus, derivatives **Py0Me₂Fu** and **Py1Me₂Fu** can be compared to their previously reported analogues with TCF,^{10b} **Py0TCF** and **Py1TCF** respectively (Figures 7 and 8). For the shorter derivatives **0**, and in consequence, with more polarized structures, a higher nonlinearity, which is accompanied by a hypsochromic shift of the absorption bands is found for **Py0Me₂Fu**. For derivatives **1**, with less polarized structures, compound **Py1TCF**, bearing the stronger acceptor shows a higher NLO response, but **Py1Me₂Fu** is also more transparent (Table 4).

Chromophores of series **Bz** show positive figure of merit $\mu\beta_0$, contrary to their equivalents with 2-dicyanomethylenethiazole as acceptor.^{11e} The latter are right-handed chromophores, with a predominantly zwitterionic form for their ground electronic state. Although these were measured in DMSO due to their limited solubility in CH₂Cl₂, the qualitative experimental results in the latter solvent also pointed to negative nonlinearities. Considering the use of different solvents, values for compounds **Bz0(PhFu,Me₂Fu,BuFu)** and **Bz1(PhFu,Me₂Fu,BuFu)** are similar or even higher in absolute values.

Further comparisons with benzothiazolylidene chromophores bearing other acceptors are somewhat restricted by the different experimental setups used in the measurement of the corresponding second-order NLO properties (Hyper Raleigh Scattering (HRS) as technique, other laser wavelength and/or other solvents)^{11b-c,32,39} or by the structure of merocyanine featuring a quite different π -spacer.^{11d}

Thus, in short, the NLO properties of furanone-containing merocyanines herein studied compare favorably to those of related chromophores bearing more efficient acceptor units.

Conclusion

$\Delta^{\alpha,\beta}$ -butenolides (or 2(5*H*)-furanones) have been used as acceptor ends in the synthesis of D- π -A systems with second-order NLO properties. All derivatives exist as a resonance hybrid of the neutral and zwitterionic forms, with different molecular polarization (and thus, different properties), depending on the donor unit and the butenolide fragment.

X-ray crystallography, NMR data and calculated NBO charges reveal that polarization of the chromophores studied increases in the order: systems **Me₂Fu** < systems **BuFu** < systems **PhFu**. Moreover, derivatives of proaromatic butenolide **PhFu** show the easiest reduction process and the highest absorption wavelength.

The benzothiazolylidene moiety has a better electron-donating ability compared to that of the pyranilylidene ring, as disclosed by X-ray studies, theoretical data, IR, Raman and CV. This fact gives rise to a more effective polarization for chromophores of **Bz** series with an important contribution, for compounds bearing the proaromatic furanones **PhFu**, **BuFu**, of the canonical form in which furan gets aromatic. Furthermore, unlike most D- π -A systems,

the degree of ICT in derivatives **Bz** increases on lengthening the π -spacer, as revealed by IR and Raman spectroscopies.

All compounds display positive $\mu\beta_0$ values, showing chromophores endowed with the proaromatic butenolide **PhFu** as acceptor moiety the best NLO responses. The change **Py** \rightarrow **Bz** results in lower second-order nonlinearities **for derivatives 0**, due to the more polarized structures for derivatives **Bz**. Incorporation of furanones **PhFu, Me₂Fu, BuFu** leads to moderately-polarized structures with higher NLO responses (accompanied sometimes by a better transparency) when compared to other chromophores bearing more efficient acceptors. Taking these data into account, 2(5*H*)-furanones become suitable acceptor moieties for the preparation of novel structures with an effective **polarization** and upgraded second-order NLO responses.

Experimental Section

General information: See the Supporting Information.

Starting materials: Compounds **PhFu**,¹⁴ **Py0**,¹⁷ **Py1**,^{10b} **Bz0**,²⁰ and **Bz1**²⁰ were prepared as previously described. Acceptor **Me₂Fu** was prepared by following the same procedure reported for the corresponding analogue with methyl and ethyl groups in C5.^{15b}

4-tert-butyl-2-oxo-2,5-dihydrofuran-3-carbonitrile (BuFu). 1-bromopinacolone (2 mL, 14.9 mmol) and cyanoacetic acid (1.26 g, 14.9 mmol) were added to a solution of NaOH (0.60 g, 14.9 mmol) in ethanol/water (22 mL/5 mL) under an argon atmosphere. The reaction mixture was heated at reflux for 6h30min (TLC monitoring). The final red solution was evaporated and the crude product dissolved in EtOAc (20 mL). The organic layer was washed with water (2 \times 10 mL), dried over MgSO₄ and evaporated. The resulting orange oil

was purified by flash chromatography (silica gel) with CH₂Cl₂ as the eluent, obtaining first, compound **BuFu** (4-*tert*-butyl-2-oxo-2,5-dihydrofuran-3-carbonitrile: 884 mg, 36%) as a yellow oil which solidified on standing, then **1** (3,3-dimethyl-2-oxobutyl cyanoacetate: 317 mg, 10%) as a yellowish solid. A second fraction of compound **BuFu** was obtained by cyclisation of **1** as follows: 3,3-dimethyl-2-oxobutyl cyanoacetate **1** (317 mg, 1.73 mmol) was added to a solution of Na (20 mg, 0.87 mmol) in EtOH (2 mL) under an argon atmosphere. The mixture was stirred for 24h turning from orange to red. HCl 1N (2.9 mL, 2.9 mmol) was added, and the aqueous layer was extracted with CH₂Cl₂ (3×10 mL), and the resulting organic layer was dried over MgSO₄ and evaporated. The crude oil was purified by flash chromatography (silica gel) with CH₂Cl₂/hexane 9.5:0.5 as the eluent to give **BuFu** (57 mg, 20%).

4-*tert*-butyl-2-oxo-2,5-dihydrofuran-3-carbonitrile (BuFu). Mp 60–63 °C (Ref.¹⁶: mp 64 °C); ¹H NMR (400 MHz, CDCl₃): δ = 4.98 (s, 2H), 1.41 ppm (s, 9H); ¹³C NMR (75 MHz, CDCl₃): δ = 188.2, 168.0, 111.1, 110.0, 71.1, 35.4, 28.4 ppm; IR (neat): $\bar{\nu}$ = 2975 (C_{sp3}-H), 2238 (C≡N), 1776 (C=O), 1626 cm⁻¹ (C=C); HRMS (ESI⁺): *m/z* [M+H]⁺ calcd for C₉H₁₂NO₂ 166.0863; found 166.0894; [M+Na]⁺ calcd for C₉H₁₁NNaO₂ 188.0682; found 188.0698; **Anal. Calcd for C₉H₁₁NO₂: C 65.44, H 6.71, N 8.48. Found: C 65.19, H 6.50, N,**

8.56.

3,3-dimethyl-2-oxobutyl cyanoacetate (1). Mp 46–51 °C; ¹H NMR (400 MHz, CDCl₃): δ = 4.99 (s, 2H), 3.60 (s, 2H), 1.20 ppm (s, 9H); ¹³C NMR (100 MHz, CDCl₃): δ = 206.3, 162.6, 112.7, 66.1, 42.7, 26.0, 24.3 ppm; IR (Nujol): $\bar{\nu}$ = 2261 (C≡N), 1759 (C=O), 1724 cm⁻¹ (C=O); HRMS (ESI⁺): *m/z* [M+Na]⁺ calcd for C₉H₁₃NNaO₃ 206.0788; found

206.0772; Anal. Calcd for C₉H₁₃NO₃: C 59.00, H 7.15, N 7.65. Found: C 58.75, H 7.32, N, 7.85.

Compounds Py0(PhFu,Me₂Fu,BuFu). *General procedure.* To a solution of aldehyde **Py0** (111 mg, 0.48 mmol) in absolute ethanol (5 mL) the corresponding acceptor (**PhFu,Me₂Fu,BuFu**) (0.48 mmol) was added. (For the reaction with acceptor **Me₂Fu** piperidine (one drop) was added). The mixture was refluxed under argon with exclusion of light (TLC monitoring). In the case of **Py0PhFu** and **Py0Me₂Fu**, after cooling, the resulting solid was isolated by filtration, washed with cold ethanol and a cold mixture of pentane/CH₂Cl₂ 9.5:0.5. In the case of **Py0BuFu**, the solvent was evaporated and the crude product was purified by flash chromatography (silica gel).

(Z)-5-(2-(2,6-di-tert-butyl-4H-pyran-4-ylidene)ethylidene)-2-oxo-4-phenyl-2,5-dihydrofuran-3-carbonitrile (Py0PhFu). Reaction time: 5 hours. Evaporation of the filtrate and flash chromatography (silica gel) with CH₂Cl₂ as the eluent gave a second fraction. Yield: dark blue solid (118 mg; 62%). Mp 241–246 °C; ¹H NMR (400 MHz, CDCl₃): δ = 7.62–7.53 (m, 5H), 6.67 (d, *J* = 13.1 Hz, 1H), 6.18 (d, *J* = 1.8 Hz, 1H), 6.13 (d, *J* = 13.1 Hz, 1H), 6.07 (d, *J* = 1.8 Hz, 1H), 1.26 (s, 9H), 1.24 ppm (s, 9H); ¹³C NMR (100 MHz, CDCl₃): δ = 169.6, 169.3, 165.7, 157.6, 145.2, 141.3, 131.1, 129.2, 128.9, 120.8, 114.0, 113.7, 108.5, 107.5, 100.3, 91.1, 36.3, 36.1, 27.8 ppm; IR (Nujol): $\bar{\nu}$ = 2213 (C≡N), 1739 (C=O), 1655 (C=C), 1589 (C=C), 1567 cm⁻¹ (C=C); HRMS (ESI⁺): *m/z* [M+H]⁺ calcd for C₂₆H₂₈NO₃ 402.2064; found 402.2062; [M+Na]⁺ calcd for C₂₆H₂₇NNaO₃ 424.1883; found 424.1861; [2M+H]⁺ calcd for C₅₂H₅₅N₂O₆ 803.4055; found 803.4050; [2M+Na]⁺ calcd for C₅₂H₅₄N₂NaO₆ 825.3874; found 825.3862; Anal. Calcd for C₂₆H₂₇NO₃: C 77.78, H 6.78, N 3.49. Found: C 78.01, H 6.54, N 3.71.

(E)-4-(3-(2,6-di-*tert*-butyl-4*H*-pyran-4-ylidene)prop-1-enyl)-5,5-dimethyl-2-oxo-2,5-dihydrofuran-3-carbonitrile (Py0Me₂Fu). Reaction time: 16h30min. Evaporation of the filtrate and flash chromatography (silica gel) with CH₂Cl₂ as the eluent gave a second fraction. Yield: bright dark violet solid (122 mg; 69%). Mp 203–206 °C; ¹H NMR (400 MHz, CDCl₃): δ = 8.36 (dd, *J*₁ = 14.5 Hz, *J*₂ = 12.4 Hz, 1H), 6.47 (d, *J* = 1.9 Hz, 1H), 5.96 (d, *J* = 1.9 Hz, 1H), 5.79 (d, *J* = 14.5 Hz, 1H), 5.68 (d, *J* = 12.4 Hz, 1H), 1.52 (s, 6H), 1.28 (s, 9H), 1.25 ppm (s, 9H); ¹³C NMR (100 MHz, CDCl₃): δ = 176.4, 169.0, 168.9, 168.3, 145.6, 143.8, 115.6, 111.7, 108.9, 106.4, 100.7, 87.1, 86.0, 36.2, 36.0, 27.8, 26.0 ppm; IR (Nujol): $\bar{\nu}$ = 2206 (C≡N), 1738 (C=O), 1661 (C=C), 1596 (C=C), 1544 cm⁻¹ (C=C); HRMS (ESI⁺): *m/z* [M+H]⁺ calcd for C₂₃H₃₀NO₃ 368.2220; found 368.2196; [M+Na]⁺ calcd for C₂₃H₂₉NNaO₃ 390.2040; found 390.2012; Anal. Calcd for C₂₃H₂₉NO₃: C 75.17, H 7.95, N 3.81. Found: C 75.03, H 8.13, N, 4.06.

(Z)-4-*tert*-butyl-5-(2-(2,6-di-*tert*-butyl-4*H*-pyran-4-ylidene)ethylidene)-2-oxo-2,5-dihydrofuran-3-carbonitrile (Py0BuFu). Reaction time: 5h30min. Eluent chromatography: CH₂Cl₂/Et₂O 9.9:0.1. After column, the resulting solid was washed with a cold mixture of pentane/CH₂Cl₂ 9.5:0.5. Yield: dark violet solid (50 mg; 28%). Mp 226–229 °C; ¹H NMR (400 MHz, CDCl₃): δ = 6.98 (d, *J* = 12.6 Hz, 1H), 6.20 (d, *J* = 1.9 Hz, 1H), 6.04 (d, *J* = 12.6 Hz, 1H), 6.01 (d, *J* = 1.9 Hz, 1H), 1.55 (s, 9H), 1.28 (s, 9H), 1.25 ppm (s, 9H); ¹³C NMR (100 MHz, CDCl₃): δ = 168.9, 168.5, 167.7, 166.1, 143.7, 141.2, 120.7, 114.6, 107.8, 107.1, 99.7, 93.5, 36.2, 36.0, 35.1, 31.3, 27.8 ppm; IR (Nujol): $\bar{\nu}$ = 2215 (C≡N), 1746 (C=O), 1659 (C=C), 1588 (C=C), 1574 (C=C), 1512 cm⁻¹ (C=C); HRMS (ESI⁺): *m/z* [M+H]⁺ calcd for C₂₄H₃₂NO₃ 382.2377; found 382.2362; [M+Na]⁺ calcd for C₂₄H₃₁NNaO₃ 404.2196; found 404.2174; [M+K]⁺ calcd for C₂₄H₃₁KNO₃

420.1936; found 420.1922; Anal. Calcd for C₂₄H₃₁NO₃: C 75.56, H 8.19, N 3.67. Found: C 75.34, H 7.98, N, 3.83.

Compounds Py1(PhFu,Me₂Fu,BuFu). *General procedure*. To a solution of aldehyde **Py1** (110 mg, 0.42 mmol) in absolute ethanol (5 mL) the corresponding acceptor **(PhFu,Me₂Fu,BuFu)** (0.42 mmol) was added. (For the reaction with acceptor **Me₂Fu** piperidine (one drop) was added). The mixture was refluxed under argon with exclusion of light (TLC monitoring). After cooling, the solvent was evaporated and the crude product was purified by flash chromatography (silica gel) with CH₂Cl₂ as the eluent. The resulting solid was washed with a cold mixture of pentane/CH₂Cl₂ 9.5:0.5.

(Z)-5-((E)-4-(2,6-di-*tert*-butyl-4*H*-pyran-4-ylidene)but-2-enylidene)-2-oxo-4-phenyl-2,5-dihydrofuran-3-carbonitrile (Py1PhFu). Reaction time: 8h15min. Yield: dark blue solid (43 mg; 24%). Mp 186–190 °C; ¹H NMR (400 MHz, CDCl₃): δ = 7.61–7.53 (m, 5H), 7.13 (dd, *J*₁ = 13.4 Hz, *J*₂ = 12.6 Hz, 1H), 6.65 (dd, *J*₁ = 13.4 Hz, *J*₂ = 12.2 Hz, 1H), 6.46 (dd, *J*₁ = 12.2 Hz, *J*₂ = 0.4 Hz, 1H), 6.24 (d, *J* = 1.8 Hz, 1H), 5.89 (d, *J* = 1.8 Hz, 1H), 5.73 (d, *J* = 12.6 Hz, 1H), 1.24 (s, 9H), 1.23 ppm (s, 9H); ¹³C NMR (100 MHz, CDCl₃): δ = 167.7, 167.6, 165.4, 158.1, 142.6, 142.4, 141.7, 131.2, 129.2, 128.9, 128.7, 125.9, 120.6, 114.0, 113.4, 106.5, 100.0, 92.6, 36.1, 35.9, 27.9, 27.8 ppm; IR (Nujol): $\bar{\nu}$ = 2217 (C≡N), 1742 (C=O), 1657 (C=C), 1557(C=C), 1518 cm⁻¹ (C=C); HRMS (ESI⁺): *m/z* [M+H]⁺ calcd for C₂₈H₃₀NO₃ 428.2220; found 428.2209; [M+Na]⁺ calcd for C₂₈H₂₉NNaO₃ 450.2040; found 450.2011; [M+K]⁺ calcd for C₂₈H₂₉KNO₃ 466.1779; found 466.1748; Anal. Calcd for C₂₈H₂₉NO₃: C 78.66, H 6.84, N 3.28. Found: C 78.82, H 6.74, N 3.51.

4-((1*E*,3*E*)-5-(2,6-di-*tert*-butyl-4*H*-pyran-4-ylidene)penta-1,3-dienyl)-5,5-dimethyl-2-oxo-2,5-dihydrofuran-3-carbonitrile (Py1Me₂Fu). Reaction time: 9 hours. Yield: dark

green solid (33 mg; 20%). Mp 232–235 °C; ^1H NMR (400 MHz, CDCl_3): δ = 7.71 (dd, J_1 = 14.9 Hz, J_2 = 11.6 Hz, 1H), 7.19 (dd, J_1 = 13.8 Hz, J_2 = 12.5 Hz, 1H), 6.26 (d, J = 1.8 Hz, 1H), 6.22 (dd, J_1 = 13.8 Hz, J_2 = 11.6 Hz, 1H), 6.00 (d, J = 14.9 Hz, 1H), 5.83 (d, J = 1.8 Hz, 1H), 5.62 (d, J = 12.5 Hz, 1H), 1.56 (s, 6H), 1.27 (s, 9H), 1.22 ppm (s, 9H); ^{13}C NMR (100 MHz, CDCl_3): δ = 175.7, 167.8, 167.2, 166.8, 148.5, 142.4, 140.9, 125.1, 114.2, 112.6, 112.4, 106.0, 99.7, 90.3, 86.3, 36.1, 35.7, 27.9, 27.7, 26.1 ppm; IR (Nujol): $\bar{\nu}$ = 2201 (C \equiv N), 1742 (C=O), 1662 (C=C), 1576 cm^{-1} (C=C); HRMS (ESI $^+$): m/z [M+H] $^+$ calcd for $\text{C}_{25}\text{H}_{32}\text{NO}_3$ 394.2377; found 394.2378; calcd for [M+Na] $^+$ $\text{C}_{25}\text{H}_{31}\text{NNaO}_3$ 416.2196; found 416.2177; Anal. Calcd for $\text{C}_{25}\text{H}_{31}\text{NO}_3$: C 76.30, H 7.94, N 3.56. Found: C 76.45, H 7.73, N 3.83.

(Z)-4-tert-butyl-5-((E)-4-(2-(2,6-di-tert-butyl-4H-pyran-4-ylidene)but-2-enylidene)-2-oxo-2,5-dihydrofuran-3-carbonitrile (Py1BuFu). Reaction time: 9 hours. Yield: dark blue solid (39 mg; 23%). Mp 127–130 °C; ^1H NMR (400 MHz, CDCl_3): δ = 7.08 (dd, J_1 = 13.7 Hz, J_2 = 12.5 Hz, 1H), 6.73 (d, J = 11.9 Hz, 1H), 6.59 (dd, J_1 = 13.7 Hz, J_2 = 11.9 Hz, 1H), 6.23 (d, J = 1.6 Hz, 1H), 5.84 (d, J = 1.6 Hz, 1H), 5.68 (d, J = 12.5 Hz, 1H), 1.54 (s, 9H), 1.26 (s, 9H), 1.22 ppm (s, 9H); ^{13}C NMR (100 MHz, CDCl_3): δ = 168.3, 167.0, 166.8, 165.7, 142.5, 140.9, 140.3, 125.7, 120.5, 114.2, 113.7, 106.2, 99.7, 95.1, 36.1, 35.8, 31.2, 29.7, 27.9, 27.8 ppm; IR (Nujol): $\bar{\nu}$ = 2219 (C \equiv N), 1749 (C=O), 1659 (C=C), 1558 cm^{-1} (C=C); HRMS (ESI $^+$): m/z [M+H] $^+$ calcd for $\text{C}_{26}\text{H}_{34}\text{NO}_3$ 408.2533; found 408.2514; [M+Na] $^+$ calcd for $\text{C}_{26}\text{H}_{33}\text{NNaO}_3$ 430.2353; found 430.2323; [M+K] $^+$ calcd for $\text{C}_{26}\text{H}_{33}\text{KNO}_3$ 446.2092; found 446.2055; Anal. Calcd for $\text{C}_{26}\text{H}_{33}\text{NO}_3$: C 76.62, H 8.16, N 3.44. Found: C 76.39, H 8.45, N 3.66.

Compounds Bz0(PhFu,Me₂Fu,BuFu). *General procedure.* To a solution of benzothiazolium salt **Bz0** (60 mg; 0.15 mmol) and the corresponding acceptor (**PhFu,Me₂Fu,BuFu**) (0.15 mmol) in ethanol (1.6 mL), triethylamine (0.27 mL, 1.94 mmol) was added. The mixture was refluxed under argon with exclusion of light (TLC monitoring). In the case of **Bz0PhFu**, after cooling, the resulting solid was isolated by filtration, washed with cold ethanol and a cold mixture of pentane/CH₂Cl₂ 9.5:0.5. In the case of **Bz0Me₂Fu,Bz0BuFu**, the solvent was evaporated and the crude product was purified by flash chromatography (silica gel).

(Z)-5-((Z)-2-(3-ethylbenzothiazol-2(3H)-ylidene)ethylidene)-2-oxo-4-phenyl-2,5-dihydrofuran-3-carbonitrile (Bz0PhFu). Reaction time: 25 min. Yield: violet to greyish solid (32 mg; 59%). Mp 291–293 °C (Ref. ¹⁴: mp 279–281 °C); ¹H NMR (400 MHz, CDCl₃): δ = 7.63–7.53 (m, 5H), 7.50 (dd, *J*₁ = 7.9 Hz, *J*₂ = 1.0 Hz, 1H), 7.42 (ddd, *J*₁ = 8.4 Hz, *J*₂ = 7.6 Hz, *J*₃ = 1.0 Hz, 1H), 7.23 (ddd, *J*₁ = 7.9 Hz, *J*₂ = 7.6 Hz, *J*₃ = 0.9 Hz, 1H), 7.17 (dd, *J*₁ = 8.4 Hz, *J*₂ = 0.9 Hz, 1H), 6.62 (d, *J* = 12.6 Hz, 1H), 6.22 (d, *J* = 12.6 Hz, 1H), 4.14 (q, *J* = 7.3 Hz, 2H), 1.44 ppm (t, *J* = 7.3 Hz, 3H); ¹³C NMR (100 MHz, CDCl₃): δ = 166.7, 160.0, 155.4, 141.2, 138.3, 130.8, 129.4, 129.2, 128.9, 127.7, 124.7, 124.3, 123.8, 122.2, 114.5, 111.1, 104.7, 92.2, 41.0, 12.2 ppm; IR (Nujol): $\bar{\nu}$ = 2207 (C≡N), 1722 (C=O), 1691 (C=C), 1594 (C=C), 1576 (C=C), 1531 cm⁻¹ (C=C); HRMS (ESI⁺): *m/z* [M+H]⁺ calcd for C₂₂H₁₇N₂O₂S 373.1005; found 373.0988; [M+Na]⁺ calcd for C₂₂H₁₆N₂NaO₂S 395.0825; found 395.0803; Anal. Calcd for C₂₂H₁₆N₂O₂S: C 70.95, H 4.33, N 7.52. Found: C 71.04, H 4.05, N 7.58.

4-((1E,3Z)-3-(3-ethylbenzothiazol-2(3H)-ylidene)prop-1-enyl)-5,5-dimethyl-2-oxo-2,5-dihydrofuran-3-carbonitrile (Bz0Me₂Fu). Reaction time: 35 min. Eluent

chromatography: CH₂Cl₂/Et₂O 9.6:0.4. Yield: dark violet solid (26 mg; 52%). Mp 248–251 °C; ¹H NMR (400 MHz, CD₃COCD₃): δ = 8.12 (dd, *J*₁ = 13.8 Hz, *J*₂ = 12.6 Hz, 1H), 7.85 (ddd, *J*₁ = 7.9 Hz, *J*₂ = 1.1 Hz, *J*₃ = 0.6 Hz, 1H), 7.52–7.45 (m, 2H), 7.30 (ddd, *J*₁ = 7.9 Hz, *J*₂ = 6.1 Hz, *J*₃ = 2.3 Hz, 1H), 6.20 (d, *J* = 12.6 Hz, 1H), 5.97 (d, *J* = 13.8 Hz, 1H), 4.31 (q, *J* = 7.2 Hz, 2H), 1.53 (s, 6H), 1.41 ppm (t, *J* = 7.2 Hz, 3H); ¹³C NMR (100 MHz, CD₃COCD₃): δ = 177.1, 170.0, 147.3, 143.4, 129.4, 126.8, 125.8, 124.4, 124.1, 118.1, 113.5, 106.6, 96.8, 87.1, 42.5, 27.7, 13.4 ppm; IR (Nujol): $\bar{\nu}$ = 2210 (C≡N), 1723 (C=O), 1581 (C=C), 1562 cm⁻¹ (C=C); HRMS (ESI⁺): *m/z* [M+H]⁺ calcd for C₁₉H₁₉N₂O₂S 339.1162; found 339.1136; [M+Na]⁺ calcd for C₁₉H₁₈N₂NaO₂S 361.0981; found 361.0945; Anal. Calcd for C₁₉H₁₈N₂O₂S: C 67.43, H 5.36, N 8.28. Found: C 67.65, H 5.05, N 8.49.

(Z)-5-((Z)-2-(3-ethylbenzothiazol-2(3H)-ylidene)ethylidene)-2-oxo-4-tert-butyl-2,5-dihydrofuran-3-carbonitrile (Bz0BuFu). Reaction time: 75 min. Eluent chromatography: CH₂Cl₂/Et₂O 9.3:0.7. The solid obtained by flash chromatography was further washed with a mixture of pentane/CH₂Cl₂ 8.5/1.5. Yield: purple-violet solid (8 mg; 15%). Mp 265–268 °C; ¹H NMR (400 MHz, CD₂Cl₂): δ = 7.55 (dd, *J*₁ = 7.8 Hz, *J*₂ = 1.0 Hz, 1H), 7.42 (ddd, *J*₁ = 8.3 Hz, *J*₂ = 7.8 Hz, *J*₃ = 1.0 Hz, 1H), 7.23 (td, *J*₁ = 7.8 Hz, *J*₂ = 1.0 Hz, 1H), 7.18 (d, *J* = 8.3 Hz, 1H), 7.03 (d, *J* = 12.4 Hz, 1H), 6.11 (d, *J* = 12.4 Hz, 1H), 4.13 (q, *J* = 7.3 Hz, 2H), 1.55 (s, 9H), 1.41 ppm (t, *J* = 7.3 Hz, 3H); ¹³C NMR: not registered due to its low solubility; IR (Nujol): $\bar{\nu}$ = 2209 (C≡N), 1720 (C=O), 1591 (C=C), 1531 cm⁻¹ (C=C); HRMS (ESI⁺): *m/z* [M+Na]⁺ calcd for C₂₀H₂₀N₂NaO₂S 375.1138; found 375.1140; Anal. Calcd for C₂₀H₂₀N₂O₂S: C 68.16, H 5.72, N 7.95. Found: C 68.34, H 5.42, N 7.80.

Compounds Bz1(PhFu,Me₂Fu,BuFu). *General procedure*. To a solution of benzothiazolium salt **Bz1** (334 mg; 0.70 mmol) and the corresponding acceptor

(**PhFu,Me₂Fu,BuFu**) (0.70 mmol) in ethanol (7.5 mL), triethylamine (1.3 mL, 9.32 mmol) was added. The mixture was refluxed under argon with exclusion of light (TLC monitoring). After cooling, the resulting solid was isolated by filtration, washed with cold ethanol and a cold mixture of pentane/CH₂Cl₂ 9.5/0.5 and finally purified by flash chromatography (silica gel) with CH₂Cl₂/Et₂O 8:2 (9.2:0.8 for **Bz1Me₂Fu**) as the eluent.

(Z)-5-((2E,4Z)-4-(3-ethylbenzothiazol-2(3H)-ylidene)but-2-enylidene)-2-oxo-4-phenyl-2,5-dihydrofuran-3-carbonitrile (Bz1PhFu). Reaction time: 25 min. The solid obtained by flash chromatography was further washed with a mixture of pentane/CH₂Cl₂ 7.5/2.5. Yield: Blue-green solid (81 mg; 29%). Mp 272–275 °C; ¹H NMR (400 MHz, CD₂Cl₂): 7.63–7.54 (m, 5H), 7.52 (d, *J* = 7.8 Hz, 1H), 7.39 (t, *J* = 7.8 Hz, 1H), 7.19 (t, *J* = 7.8 Hz, 1H), 7.16–7.07 (m, 2H), 6.64–6.53 (m, 2H), 5.96 (d, *J* = 12.2 Hz, 1H), 4.05 (q, *J* = 7.2 Hz, 2H), 1.39 ppm (t, *J* = 7.2 Hz, 3H); ¹³C NMR: not registered due to its low solubility; IR (Nujol): $\bar{\nu}$ = 2200 (C≡N), 1729 (C=O), 1556 cm⁻¹ (C=C); HRMS (ESI⁺): *m/z* [M]⁺ calcd for C₂₄H₁₈N₂O₂S 398.1083; found 398.1084; [M+Na]⁺ calcd for C₂₄H₁₈N₂NaO₂S 421.0981; found 421.0981; Anal. Calcd for C₂₄H₁₈N₂O₂S: C 72.34, H 4.55, N 7.03. Found: C 72.51, H 4.34, N 6.93.

4-((2E,4Z)-4-(3-ethylbenzothiazol-2(3H)-ylidene)but-2-enylidene)-5,5-dimethyl-2-oxo-2,5-dihydrofuran-3-carbonitrile (Bz1Me₂Fu). Reaction time: 1 hour. A further purification by flash chromatography on reverse C18 silica gel, with acetonitrile/aqueous CH₃COONH₄ 15 mM from 6:4 to 10:0 was needed. Yield: Deep blue solid (40 mg; 16%). Mp 254–259 °C; ¹H NMR (300 MHz, CD₂Cl₂): δ = 7.63 (dd, *J*₁ = 14.6 Hz, *J*₂ = 11.7 Hz, 1H), 7.49 (dd, *J*₁ = 7.7 Hz, *J*₂ = 1.0 Hz, 1H), 7.34 (ddd, *J*₁ = 8.2 Hz, *J*₂ = 7.7 Hz, *J*₃ = 1.0 Hz, 1H), 7.14 (td, *J*₁ = 7.7 Hz, *J*₂ = 1.0 Hz, 1H), 7.11 (d, *J* = 13.3 Hz, 1H), 7.05 (d, *J* = 8.2

Hz, 1H), 6.22 (dd, $J_1 = 13.3$ Hz, $J_2 = 11.9$ Hz, 1H), 5.99 (d, $J = 14.6$ Hz, 1H), 5.78 (d, $J = 11.9$ Hz, 1H), 3.99 (q, $J = 7.2$ Hz, 2H), 1.56 (s, 6H), 1.36 ppm (t, $J = 7.2$ Hz, 3H); ^{13}C NMR: not registered due to its low solubility; IR (Nujol): $\bar{\nu} = 2213$ (C \equiv N), 1739 (C=O), 1651, 1581 cm^{-1} (C=C); HRMS (ESI $^+$): m/z [M+Na] $^+$ calcd for C $_{21}$ H $_{20}$ N $_2$ NaO $_2$ S 387.1138; found 387.1144; Anal. Calcd for C $_{21}$ H $_{20}$ N $_2$ O $_2$ S: C 69.21, H 5.53, N 7.69. Found: C 69.10, H 5.41, N 7.80.

(Z)-4-tert-butyl-5-((2E,4Z)-4-(3-ethylbenzothiazol-2(3H)-ylidene)but-2-enylidene)-2-oxo-2,5-dihydrofuran-3-carbonitrile (Bz1BuFu). Reaction time: 1 hour. Yield: Blue-green solid (44 mg; 17%). Mp 241–245 °C; ^1H NMR (400 MHz, THF- d_8): $\delta = 7.51$ (dd, $J_1 = 7.8$ Hz, $J_2 = 1.2$ Hz, 1H), 7.31 (ddd, $J_1 = 8.2$ Hz, $J_2 = 7.4$ Hz, $J_3 = 1.2$ Hz, 1H), 7.19 (dd, $J_1 = 8.2$ Hz, $J_2 = 0.4$ Hz, 1H), 7.13–7.05 (m, 2H), 6.93 (dd, $J_1 = 11.8$ Hz, $J_2 = 0.6$ Hz, 1H), 6.52 (dd, $J_1 = 13.6$ Hz, $J_2 = 11.8$ Hz, 1H), 6.03 (d, $J = 11.8$ Hz, 1H), 4.08 (q, $J = 7.2$ Hz, 2H), 1.51 (s, 9H), 1.32 ppm (t, $J = 7.2$ Hz, 3H); ^{13}C NMR: not registered due to its low solubility; IR (Nujol): $\bar{\nu} = 2191$ (C \equiv N), 1702 (C=O), 1562 cm^{-1} (C=C); HRMS (ESI $^+$): m/z [M] $^+$ calcd for C $_{22}$ H $_{22}$ N $_2$ O $_2$ S 378.1397; found 378.1393; [M+Na] $^+$ calcd for C $_{22}$ H $_{22}$ N $_2$ NaO $_2$ S 401.1294; found 401.1299; Anal. Calcd for C $_{22}$ H $_{22}$ N $_2$ O $_2$ S: C 69.81, H 5.86, N 7.40. Found: C 70.10, H 5.65, N 7.56.

Acknowledgments. We thank Dr. E. Galán (Delft University of Technology, The Netherlands) for helpful discussions. Financial support from MICINN-FEDER (CTQ2011-22727 and MAT2011-27978-C02-02), MINECO (CTQ2014-52331R) and Gobierno de Aragón-Fondo Social Europeo (E39 and E04) is gratefully acknowledged. Research at the Universidad de Málaga was supported by MINECO (CTQ2012-33733) and Junta de

Andalucía (P09-4708). Authors would like to acknowledge the use of Servicio General de Apoyo a la Investigación-SAI, Universidad de Zaragoza.

Supporting Information Available. General experimental methods, NMR and UV–vis spectra of new compounds, NLO measurements, X-ray crystallographic data in CIF format and diagram of the crystal structures of **Py0PhFu**, **Py1PhFu**, **Py1Me₂Fu** and **Bz0PhFu**, computed energies and Cartesian coordinates of optimized geometries, and contour plots of frontier molecular orbitals of all chromophores with the exception of **Py1BuFu**. This material is available free of charge via the Internet at <http://pubs.acs.org>.

References and Footnotes

(1) (a) Themed issue on Organic Nonlinear Optics: Marder, S. R. (Guest Ed.), *J. Mater. Chem.* **2009**, *19* (40). (b) Dalton, L. R.; Sullivan, P. A.; Bale, D. H. *Chem. Rev.* **2010**, *110*, 25–55. (c) Stegeman, G. I.; Stegeman R. A. in *Nonlinear Optics: Phenomena, Materials, and Devices*, (Ed.: Boreman, G.), Wiley Series in Pure and Applied Optics, John Wiley & Sons: Hoboken, **2012**. (d) Coe, B. J. *Coord. Chem. Rev.* **2013**, *257*, 1438–1458. (e) Castet, F.; Rodriguez, V.; Pozzo, J.-L.; Ducasse, L.; Plaquet, A.; Champagne, B. *Acc. Chem. Res.* **2013**, *46*, 2656–2665.

(2) Bureš, F. *RSC Adv.* **2014**, *4*, 58826–58851, and references cited therein.

(3) (a) Marder, S. R.; Perry, J. W.; Tiemann, B. G.; Gorman, C. B.; Gilmour, S.; Biddle, S. L.; Bourhill, G. *J. Am. Chem. Soc.* **1993**, *115*, 2524–2526. (b) Bourhill, G.; Brédas, J.-L.; Cheng, L.-T.; Marder, S. R.; Meyers, F.; Perry, J. W.; Tiemann, B. G. *J. Am. Chem. Soc.* **1994**, *116*, 2619–2620.

(4) (a) Marder, S. R.; Beratan, D. N.; Cheng, L.-T. *Science* **1991**, *252*, 103–106. (b) Gorman, C. B.; Marder, S. R. *Proc. Natl. Acad. Sci. USA* **1993**, *90*, 11297–11301. (c) Meyers, F.; Marder, S. R.; Pierce, B. M.; Brédas, J.-L. *J. Am. Chem. Soc.* **1994**, *116*, 10703–10714. (d) Marder, S. R.; Gorman, C. B.; Meyers, F.; Perry, J. W.; Bourhill, G.; Brédas, J.-L.; Pierce, B. M. *Science* **1994**, *265*, 632–635.

(5) (a) Stiegman, A. E.; Graham, E.; Perry, K. J.; Khundkar, L. R.; Cheng, L.-T.; Perry, J. W. *J. Am. Chem. Soc.* **1991**, *113*, 7658–7666. (b) Cheng, L.-T.; Tam, W.; Marder, S. R.; Stiegman, A. E.; Rikken, G.; Spangler, C. W. *J. Phys. Chem.* **1991**, *95*, 10643–10652. (c) de Lucas, A. I.; Martín, N.; Sánchez, L.; Seoane, C.; Andreu, R.; Garín, J.; Orduna, J.; Alcalá, R.; Villacampa, B. *Tetrahedron* **1998**, *54*, 4655–4662. (d) Moreno-Mañas, M.; Pleixats, R.; Andreu, R.; Garín, J.; Orduna, J.; Villacampa, B.; Levillain, E.; Sallé, M. J. *Mater. Chem.* **2001**, *11*, 374–380. (e) González, M.; Segura, J. L.; Seoane, C.; Martín, N.; Garín, J.; Orduna, J.; Alcalá, R.; Villacampa, B.; Hernández V.; López Navarrete, J. T. *J. Org. Chem.* **2001**, *66*, 8872–8882.

(6) The term “butenolide” for describing buteno- or crotonolactones was first employed by Klobb in 1898: Klobb, T. *Bull. Soc. Chim. Fr.* **1898**, 389. Though the butenolide nomenclature has been in vogue for quite sometime, Chemical Abstracts currently has adopted the furanone system for naming these compounds. Thus, $\Delta^{\alpha,\beta}$ -butenolides are 2(5*H*)-furanones. In this article, the terms butenolide/furanone will be used interchangeably.

(7) (a) Rao, Y. S. *Chem. Rev.* **1976**, *76*, 625–694. (b) Carter, N. B.; Nadany, A. E.; Sweeny, J. B. *J. Chem. Soc., Perkin Trans. 1* **2002**, 2324–2342. (c) Ugurchieva, T. M.; Veselovsky, V. V. *Russ. Chem. Rev.* **2009**, *78*, 337–373.

(8) (a) Wang, P.; Chang, Y.; Xu, Y.; Ye, C. *Proc. SPIE-Int. Soc. Opt. Eng.* **1998**, *3556*, 73–83. (b) Asthana, D.; Ajayakumar, M. R.; Pant, R. P.; Mukhopadhyay, P. *Chem. Commun.* **2012**, *48*, 6475–6477.

(9) (a) Zhang, C.; Dalton, L. R.; Oh, M.-C.; Zhang, H.; Steier, W. H. *Chem. Mater.* **2001**, *13*, 3043–3050. (b) Liao, Y.; Eichinger, B. E.; Firestone, K. A.; Haller, M.; Luo, J.; Kaminsky, W.; Benedict, J. B.; Reid, P. J.; Jen, A. K-Y; Dalton, L. R.; Robinson, B. H. *J. Am. Chem. Soc.* **2005**, *127*, 2758–2766.

(10) Selected examples for 4*H*-pyranylidene-containing chromophores: (a) Faux, N.; Caro, B.; Robin-le Guen, F.; Le Poul, P.; Nakatani, K.; Ishow, E. *J. Organomet. Chem.* **2005**, *690*, 4982–4988. (b) Andreu, R.; Carrasquer, L.; Franco, S.; Garín, J.; Orduna, J.; Martínez de Baroja, N.; Alicante, R.; Villacampa, B.; Allain, M. *J. Org. Chem.* **2009**, *74*, 6647–6657. (c) Andreu, R.; Galán, E.; Orduna, J.; Villacampa, B.; Alicante, R.; López Navarrete, J. T.; Casado, J.; Garín, J. *Chem. –Eur. J.* **2011**, *17*, 826–838. (d) Achelle, S.; Malval, J.-P.; Aloïse, S.; Barsella, A.; Spangenberg, A.; Mager, L.; Akdas-Kilig, H.; Fillaut, J.-L.; Caro, B.; Robin-le Guen, F. *ChemPhysChem* **2013**, *14*, 2725–2736. (e) Marco, A. B.; Martínez de Baroja, N.; Franco, S.; Garín, J.; Orduna, J.; Villacampa, B.; Revuelto, A.; Andreu, R. *Chem. Asian J.* **2015**, *10*, 188–197.

(11) Selected examples: (a) Ashwell, G. J.; Malhotra, M.; Bryce, M. R.; Grainger, A. M.; *Synth. Met.* **1991**, *41–43*, 3173–3176. (b) Kay, A. J.; Woolhouse, A. D.; Gainsford, G. J.; Haskell, T. G.; Barnes, T. H.; McKinnie, I. T.; Wyss, C. P. *J. Mater. Chem.* **2001**, *11*, 996–1002. (c) Kay, A. J.; Woolhouse, A. D.; Zhao, Y.; Clays, K. *J. Mater. Chem.* **2004**, *14*, 1321–1330. (d) Latorre, S.; Moreira, I. de P. R.; Villacampa, B.; Julià, L.; Velasco, D.; Bofill, J. M.; López-Calahorra, F. *ChemPhysChem* **2010**, *11*, 912–919. (e) Andreu, R.;

Galán, E.; Garín, J.; Orduna, J.; Alicante, R.; Villacampa, B. *Tetrahedron Lett.* **2010**, *51*, 6863–6866.

(12) Selected examples: (a) Coe, B. J.; Harris, J. A.; Hall, J. J.; Brunschwig, B. S.; Hung, S.-T.; Libaers, W.; Clays, K.; Coles, S. J.; Horton, P. N.; Light, M. E.; Hursthouse, M. B.; Garín, J.; Orduna, J. *Chem. Mater.* **2006**, *18*, 5907–5918. (b) Hrobárik, P.; Sigmundová, I.; Zahradník, P.; Kasák, P.; Arion, V.; Franz, E.; Clays, K. *J. Phys. Chem. C* **2010**, *114*, 22289–22302. (c) Hrobárik, P.; Hrobáriková, V.; Sigmundová, I.; Zahradník, P.; Fakis, M.; Polyzos, I.; Persephonis, P. *J. Org. Chem.* **2011**, *76*, 8726–8736. (d) Raposo, M. M. M.; Castro, M. C. R.; Belsley, M.; Fonseca, A. M. C. *Dyes Pigm.* **2011**, *91*, 454–465.

(13) Hrobárik, P.; Zahradník, P.; Fabian, W. M. F. *Phys. Chem. Chem. Phys.* **2004**, *6*, 495–502.

(14) Acceptor **PhFu**: Ford, J. A. Jr.; Wilson, C. V.; Young, W. R. *J. Org. Chem.* **1967**, *32*, 173–177.

(15) Acceptor **Me₂Fu**: (a) Cheikh, N.; Villemin, D.; Bar, N.; Lohier, J.-F.; Choukchou-Braham, N.; Mostefa-Kara, B.; Sopkova, J. *Tetrahedron* **2013**, *69*, 1234–1247. (b) For this work acceptor **Me₂Fu** was prepared by following the same procedure reported for the corresponding analogue with methyl and ethyl groups in C5: Maheut, G.; Liao, L.; Catel, J.-M.; Jaffrès, P.-A.; Villemin, D. *J. Chem. Ed.* **2001**, *78*, 654–657.

(16) Acceptor **BuFu**: Erdmann, D.; Schuehrer, K.; Koch, W.; Schneider, G. Patent DE 2116416, 1972; *Chem. Abstr.* **1973**, *78*, 16015.

(17) Andreu, R.; Galán, E.; Garín, J.; Herrero, V.; Lacarra, E.; Orduna, J.; Alicante, R.; Villacampa, B. *J. Org. Chem.* **2010**, *75*, 1684–1692.

(18) See for example: (a) Alías, S.; Andreu, R.; Blesa, M. J.; Cerdán, M. A.; Franco, S.; Garín, J.; López, C.; Orduna, J.; Sanz, J.; Alicante, R.; Villacampa, B.; Allain, M. *J. Org.*

Chem. **2008**, *73*, 5890–5898. (b) Marco, A. B.; Andreu, R.; Franco, S.; Garín, J.; Orduna, J.; Villacampa, B.; Alicante, R. *Tetrahedron* **2013**, *69*, 3919–3926.

(19) (a) Coe, B. J.; Harris, J. A.; Asselberghs, I.; Wostyn, K.; Clays, K.; Persoons, A.; Brunshwing, B. S.; Coles, S. J.; Gelbrich, T.; Light, M. E.; Hursthouse, M. B.; Nakatani, K. *Adv. Funct. Mater.* **2003**, *13*, 347–357. (b) Beverina, L.; Fu, J.; Leclercq, A.; Zojer, E.; Pacher, P.; Barlow, S.; van Stryland, E. W.; Hagan, D. J.; Brédas, J.-L.; Marder, S. R. *J. Am. Chem. Soc.* **2005**, *127*, 7282–7283.

(20) Brooker, L. G. S.; White, F. L.; Keyes, G. H.; Smyth, C. P.; Oesper, P. F. *J. Am. Chem. Soc.* **1941**, *63*, 3192–3203.

(21) (a) Dehu, C.; Meyers, F.; Brédas, J.-L. *J. Am. Chem. Soc.* **1993**, *115*, 6198–6206. (b) Hilger, A.; Gisselbrecht, J.-P.; Tykwinski, R. R.; Boudon, C.; Schreiber, M.; Martin, R. E.; Lüthi, H. P.; Gross, M.; Diederich, F. *J. Am. Chem. Soc.* **1997**, *119*, 2069–2078.

(22) Bird, C. W. *Tetrahedron* **1986**, *42*, 89–92.

(23) Marco, A. B.; Mayorga Burrezo, P.; Mosteo, L.; Franco, S.; Garín, J.; Orduna, J.; Diosdado, B. E.; Villacampa, B.; López Navarrete, J. T.; Casado, J.; Andreu, R. *RSC Adv.* **2015**, *5*, 231–242.

(24) Chasseau, D.; Gaultier, J.; Hauw, C.; Fugnitto, R.; Gianis, V.; Strzelecka, H. *Acta Crystallogr., Sect. B: Struct. Crystallogr. Cryst. Chem.* **1982**, *38*, 1629–1631.

(25) Marder, S. R.; Cheng, L.-T.; Tiemann, B. G.; Friedli, A. C.; Blanchard-Desce, M.; Perry, J. W.; Skindhøj, J. *Science* **1994**, *263*, 511–514.

(26) Chang, Y. M. *Huaxue Tongbao* **1996**, *10*, 58–60.

(27) Poronik, Y. M.; Hugues, V.; Blanchard-Desce, M.; Gryko, D. T. *Chem. –Eur. J.* **2012**, *18*, 9258–9266.

(28) (a) Marder, S. R.; Perry, J. W.; Bourhill, G.; Gorman, C. B.; Tiemann, B. G.; Mansour, K. *Science* **1993**, *261*, 186–189. (b) For all-trans polyenes $\Delta J \sim 6.0$ Hz and for cyanines $\Delta J = 0$ Hz: Scheibe, G.; Seiffert, W.; Hohlneicher, G.; Jutz, C.; Springer, H. J. *Tetrahedron Lett.* **1966**, *7*, 5053–5059.

(29) Kulinich, A. V.; Ishchenko, A. A.; Groth, U. M. *Spectrochim. Acta, Part A* **2007**, *68*, 6–14.

(30) (a) Brooker, L. G. S.; Sklar, A. L.; Creesman, H. W. J.; Keyes, G. H.; Smith, L. A.; Sprague, R. H.; Van Lare, E.; Van Zandt, G.; White, F. L.; Williams, W. W. *J. Am. Chem. Soc.* **1945**, *67*, 1875–1889. (b) Bricks, J. L.; Kachkovskii, A. D.; Slominskii, Yu. L.; Gerasov, A. O.; Popov, S. V. *Dyes Pig.* **2015**, *121*, 238–255.

(31) Casado, J.; Moreno Oliva, M.; Ruiz Delgado, M. C.; López Navarrete, J. T.; Sánchez, L.; Martín, N.; Andreu, R.; Carrasquer, L.; Garín, J.; Orduna, J. *J. Chem. Phys.* **2007**, *126*, 074701-1–074701-8.

(32) (a) Inoue, S.; Aso, Y.; Otsubo, T. *Chem. Commun.* **1997**, 1105–1106. (b) Milián, B.; Ortí, E.; Hernández, V.; López Navarrete, J. T.; Otsubo, T. *J. Phys. Chem. B* **2003**, *107*, 12175–12183. (c) Kang, H.; Fachetti, A.; Jiang, H.; Cariati, E.; Righetto, S.; Ugo, R.; Zuccaccia, C.; Macchioni, A.; Stern, C. L.; Liu, Z.; Ho, S.-T.; Brown, E. C.; Ratner, M. A.; Marks, T. J. *J. Am. Chem. Soc.* **2007**, *129*, 3267–3286.

(33) This effect is well known as “vinylene shift”, see for example: Kachkovski, A. D.; Kovalenko, N. M. *Dyes Pig.* **1997**, *35*, 131–148.

(34) Kurdyukov, V. V.; Ishchenko, A. A.; Kudinova, M. A.; Tolmachev, A. I. *Chem. Heterocyclic Comp.* **1987**, *23*, 628–633.

(35) Ikeda, H.; Sakai, T.; Kawasaki, K. *Chem. Phys. Lett.* **1991**, *179*, 551–554.

(36) This behavior has already been reported for others D- π -A systems: (a) Ref. 23. (b) Kim, O.-K.; Fort, A.; Barzoukas, M.; Blanchard-Desce, M.; Lehn, J.-M. *J. Mater. Chem.* **1999**, *9*, 2227–2232. (c) Davies, J. A.; Elangovan, A.; Sullivan, P. A.; Olbricht, B. C.; Bale, D. H.; Ewy, T. R.; Isborn, C. M.; Eichinger, B. E.; Robinson, B. H.; Reid, P. J.; Li, X.; Dalton, L. R. *J. Am. Chem. Soc.* **2008**, *130*, 10565–10575. (d) Marco, A. B.; Andreu, R.; Franco, S.; Garín, J.; Orduna, J.; Villacampa, B.; Diosdado, B. E.; López Navarrete, J. T.; Casado, J. *Org. Biomol. Chem.* **2013**, *11*, 6338–6349.

(37) (a) Oudar, J. L.; Chemla, D. S. *J. Chem. Phys.* **1977**, *66*, 2664–2668. (b) Kanis, D. R.; Ratner, M. A.; Marks, T. J. *Chem. Rev.* **1994**, *94*, 195–242.

(38) Faux, N.; Robin-le Guen, F.; Le Poul, P.; Caro, B.; Nakatani, K.; Ishow, E.; Golhen, S. *Eur. J. Inorg. Chem.* **2006**, 3489–3497.

(39) Cho, B. R.; Je, J. T.; Lee, S. J.; Lee, S. H.; Kim, H. S.; Jeon, S. J.; Song, O.-K.; Wang, C. H. *J. Chem. Soc. Perkin Trans. 2* **1996**, 2141–2144.